

## **General Disclaimer**

### **One or more of the Following Statements may affect this Document**

- This document has been reproduced from the best copy furnished by the organizational source. It is being released in the interest of making available as much information as possible.
- This document may contain data, which exceeds the sheet parameters. It was furnished in this condition by the organizational source and is the best copy available.
- This document may contain tone-on-tone or color graphs, charts and/or pictures, which have been reproduced in black and white.
- This document is paginated as submitted by the original source.
- Portions of this document are not fully legible due to the historical nature of some of the material. However, it is the best reproduction available from the original submission.

NASA CR-159902

(NASA-CR-159902) ION PROPULSION COST  
EFFECTIVITY Final Report, 29 Mar. 1978 - 1  
Dec. 1978 (TRW Defense and Space Systems  
Group) 88 p HC A05/MF A01

CSCI 21C

N79-15153

Unclass

G3/20 43202

TRW 33590-6007-RU-00

# ION PROPULSION COST EFFECTIVITY

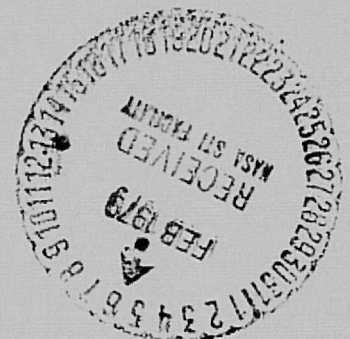
S. ZAFRAN AND J.J. BIESS  
TRW DEFENSE AND SPACE SYSTEMS GROUP  
REDONDO BEACH, CALIFORNIA 90278

December 1978

Final Report for Period 29 March - 1 December 1978

Prepared for

GODDARD SPACE FLIGHT CENTER  
Greenbelt, Maryland 20771



## ABSTRACT

Ion propulsion modules employing 8-cm thrusters and 30-cm thrusters were studied for Multimission Modular Spacecraft (MMS) applications. Recurring and nonrecurring cost elements were generated for these modules. As a result, ion propulsion cost drivers were identified to be Shuttle charges, solar array, power processing, and thruster costs. Cost effective design approaches included short length module configurations, array power sharing, operation at reduced thruster input power, simplified power processing units, and power processor output switching. The MMS mission model employed indicated that nonrecurring costs have to be shared with other programs unless the mission model grows. Extended performance missions exhibited the greatest benefits when compared with monopropellant hydrazine propulsion.<sup>1</sup>

PRECEDING PAGE BLANK

## ACKNOWLEDGEMENTS

The study effort documented herein was performed under the technical direction of Robert A. Callens, Propulsion Subsystem Technology Section Head at NASA-Goddard Space Flight Center. S. Zafran managed the study effort at TRW and performed the propulsion analysis. J. J. Biess performed the power conditioning work. Other contributions were made by G. M. Reppucci in power sources, H. F. Meissinger in spacecraft interfaces, E. E. Luedke in thermal control, and A. H. Carlin in mechanical design.

# CONTENTS

	Page
1. INTRODUCTION. . . . .	1
1.1 Study Approach . . . . .	1
1.2 Mission Selection. . . . .	1
2. HIGH PERFORMANCE PROPULSION MODULE. . . . .	5
2.1 Geosynchronous Orbit MMS Mission . . . . .	6
2.1.1 Acquisition and Reacquisition. . . . .	7
2.1.2 Stationkeeping . . . . .	7
2.1.3 Momentum Dump . . . . .	8
2.2 Low Earth Orbit MMS Mission . . . . .	8
2.3 Configuration. . . . .	9
2.3.1 8-cm Ion Thruster Power Processor. . . . .	10
2.3.2 HPPM Performance and Interface Requirements . . . . .	14
2.3.3 Propulsion Subsystem Weight. . . . .	19
2.3.4 Propulsion Subsystem Electrical Interface. . . . .	19
2.3.5 Power Subsystem Configuration . . . . .	21
2.3.6 Net Weight Impact . . . . .	22
2.4 Cost Elements . . . . .	23
2.4.1 Hardware Cost Factors . . . . .	26
2.4.2 Sensitivity Analysis . . . . .	27
2.5 Baseline Comparison with SPS . . . . .	27
2.6 Cost Reduction Studies . . . . .	31
2.6.1 Unregulated 28 Vdc Input to Power Processor. . . . .	32
2.6.2 Time Sharing DCIU. . . . .	32
2.6.3 PEU Output Switching . . . . .	33
2.6.4 Unregulated 28 Vdc Input, Time Sharing DCIU, and PEU Output Switching. . . . .	34
2.6.5 Increased Mission Life, Synchronous HPPM . . . . .	34
3. ION PROFULSION MODULE FOR SUN-SYNCHRONOUS SATELLITE SERVICING . . . . .	38
3.1 Sun-Synchronous Mission. . . . .	38
3.2 Configuration. . . . .	40
3.2.1 30-cm Ion Thruster Power Processor . . . . .	41
3.2.2 Thruster Performance Requirements. . . . .	47
3.2.3 Propulsion Module Layout and Interfaces . . . . .	48

## CONTENTS (Continued)

	Page
3.2.4 Propulsion Subsystem Weight. . . . .	52
3.2.5 Propulsion Subsystem Electrical Interface. . . . .	52
3.2.6 Power Subsystem Configuration . . . . .	53
3.2.7 Net Weight Impact . . . . .	58
3.3 Cost Elements . . . . .	59
3.3.1 Hardware Cost Factors . . . . .	61
3.3.2 Sensitivity Analysis . . . . .	61
3.4 Baseline Comparison with SPS . . . . .	63
3.5 Cost Reduction Studies . . . . .	64
3.5.1 Array Power Sharing . . . . .	64
3.5.2 Thrust Throttling . . . . .	66
3.5.3 Direct Drive (3 - Grid Thrusters) . . . . .	67
3.5.4 PPU Output Switching . . . . .	68
3.5.5 Thrust Throttling and PPU Output Switching . . . . .	68
3.5.6 Extended Sun-Synchronous Mission: Change of Local Crossing Time. . . . .	70
4. COST PROJECTION . . . . .	72
4.1 Ion Engine Programs . . . . .	72
4.2 Cost Element Projections . . . . .	73
5. CONCLUSIONS. . . . .	74
REFERENCES . . . . .	76

## ILLUSTRATIONS

		Page
1.	Ion Propulsion Cost Effectivity Study Activity Flow Diagram . . . . .	2
2.	Multimission Modular Spacecraft Bus (Exploded View) . . . .	3
3.	MMS StormSat Configuration with the HPPM . . . . .	6
4.	Possible Low Earth Orbit MMS Mission with the HPPM . . .	8
5.	Baseline Propulsion Subsystem Schematic for HPPM . . . . .	10
6.	Power Processor Functional Block Diagram . . . . .	11
7.	High Performance Propulsion Module for MMS . . . . .	17
8.	Layout of High Performance Propulsion Module with Low Earth Orbit Mission Configuration. . . . .	17
9.	Electric Power Distribution to HPPM Ion Engines . . . . .	21
10.	HPPM and SPS Sensitivity to Shuttle Price . . . . .	31
11.	Output Switching Matrix. . . . .	33
12.	Propulsion Subsystem Schematic for Sun-Synchronous Satellite Servicing . . . . .	40
13.	Electrical Prototype Power Processor for 30-cm Ion Engine Showing Modular Construction . . . . .	41
14.	Power Processor Block Diagram . . . . .	42
15.	Baseline 30-cm Thruster Power Processor Block Diagram . . . . .	45
16.	Layout of Sun-Synchronous Satellite Servicing Propulsion Module for MMS. . . . .	49
17.	Propulsion Module for Sun-Synchronous Satellite Servicing .	50
18.	Power Processor to Solar Array Interface . . . . .	55
19.	Electrical Power Interface. . . . .	57
20.	Solar Array Reconfiguration. . . . .	65
21.	Block Diagram of Power Relay Control Electronics . . . . .	66

## TABLES

		Page
1.	HPPM Missions on MMS . . . . .	5
2.	Command and Telemetry List. . . . .	13
3.	Power Processor Unit Characteristics for 8-cm Ion Thruster . . . . .	15
4.	Power Electronics Unit Part Count Analysis . . . . .	15
5.	Digital Controller and Interface Unit Part Count Analysis . .	16
6.	Ion Thruster Performance Requirements for MMS Mission . . . . .	18
7.	Ion Propulsion Subsystem Weight, Geosynchronous MMS Mission. . . . .	19
8.	Ion Propulsion Subsystem Weight, Low Earth Orbit MMS Mission. . . . .	20
9.	Ion Propulsion Subsystem Electrical Interfaces for the HPPM . . . . .	20
10.	Net Weight Impact of High Performance Propulsion Module on MMS . . . . .	22
11.	Baseline HPPM Cost Breakdown, Synchronous Mission. . .	24
12.	Baseline HPPM Cost Breakdown, Low Earth Orbit Mission.	25
13.	Sensitivity of Total Cost to HPPM Cost Elements, Synchronous Mission. . . . .	28
14.	Sensitivity of Total Cost to HPPM Cost Elements, Low Earth Orbit Mission. . . . .	29
15.	Baseline HPPM Recurring Cost Comparison with SPS (\$ Millions) . . . . .	30
16.	HPPM Cost Reduction Studies. . . . .	32
17.	HPPM (Designation 8-4) Recurring Cost Breakdown, Low Earth Orbit Mission . . . . .	35
18.	Increased Mission Life, Synchronous HPPM . . . . .	36
19.	Estimate of Baseline 30-cm Thruster Power Processor Characteristics . . . . .	46



## TABLES (Continued)

		Page
20.	Power Processing Unit Characteristics for 30-cm Ion Thruster . . . . .	47
21.	Ion Propulsion Subsystem Weight, Sun-Synchronous Satellite Servicing Mission. . . . .	52
22.	Ion Propulsion Subsystem Electrical Interface, Sun- Synchronous Satellite Servicing. . . . .	53
23.	Power Subsystem Design for the Propulsion Module— Requirements Summary. . . . .	54
24.	Power Allocation . . . . .	56
25.	Solar Array Weight Summary . . . . .	57
26.	Power Subsystem Weight Attributable to the Propulsion Module. . . . .	58
27.	Net Weight Impact of Propulsion Module for Sun- Synchronous Satellite Servicing. . . . .	59
28.	Baseline Ion Propulsion Module Cost Breakdown . . . . .	60
29.	Sensitivity of Total Cost to Ion Propulsion Module Cost Elements . . . . .	62
30.	Baseline Ion Propulsion Module Comparison with SPS-II .	63
31.	Ion Propulsion Module Cost Reduction Studies . . . . .	64
32.	Ion Module (Designation 30-5) Recurring Cost Breakdown . . . . .	69
33.	Extended Sun-Synchronous Mission Comparison. . . . .	71

## 1. INTRODUCTION

Previous studies have shown that large payload mass savings and tight pointing accuracies may be achieved through use of ion engines. In addition, because of the high specific impulse afforded by ion engines, propulsion subsystem volume reductions result from greatly reduced propellant requirements when compared to chemical systems. A recent cost comparison of candidate propulsion modules for the Multimission Modular Spacecraft (MMS) concluded that ion propulsion recurring costs are too large for it to be competitive for early MMS-Shuttle missions (Reference 1). The present need is then to show how these recurring costs can be reduced so that future Shuttle missions can realize the full potential promised by ion engines.

### 1.1 STUDY APPROACH

The study has logically been subdivided into six tasks which are illustrated in the activity flow diagram of Figure 1. Following review of the work plan with NASA-GSFC, two missions were selected from previous studies (contracts NAS 7-786 and NAS 3-20113, References 1 and 2, respectively) for further consideration. A propulsion module employing 8-cm ion engines was used for one mission, and a module employing 30-cm engines for the other. Detailed module requirements were defined which led into configurational criteria for each mission. The resulting configurations were used in the cost models for each mission, leading to identification of ion propulsion cost drivers. Study results at this point were reviewed with GSFC at an oral mid-term briefing, before proceeding into recommended methods for reducing significant costs. These reductions were summarized in cost projections for ion propulsion applications in the Shuttle era. Final study results were then reviewed and are documented in this final report together with details of work accomplished in each task.

### 1.2 MISSION SELECTION

Two missions favorable to ion propulsion were selected from References 1 and 2. The first mission is a high performance propulsion module (HPPM) for MMS that has been studied for both low-earth and orbit

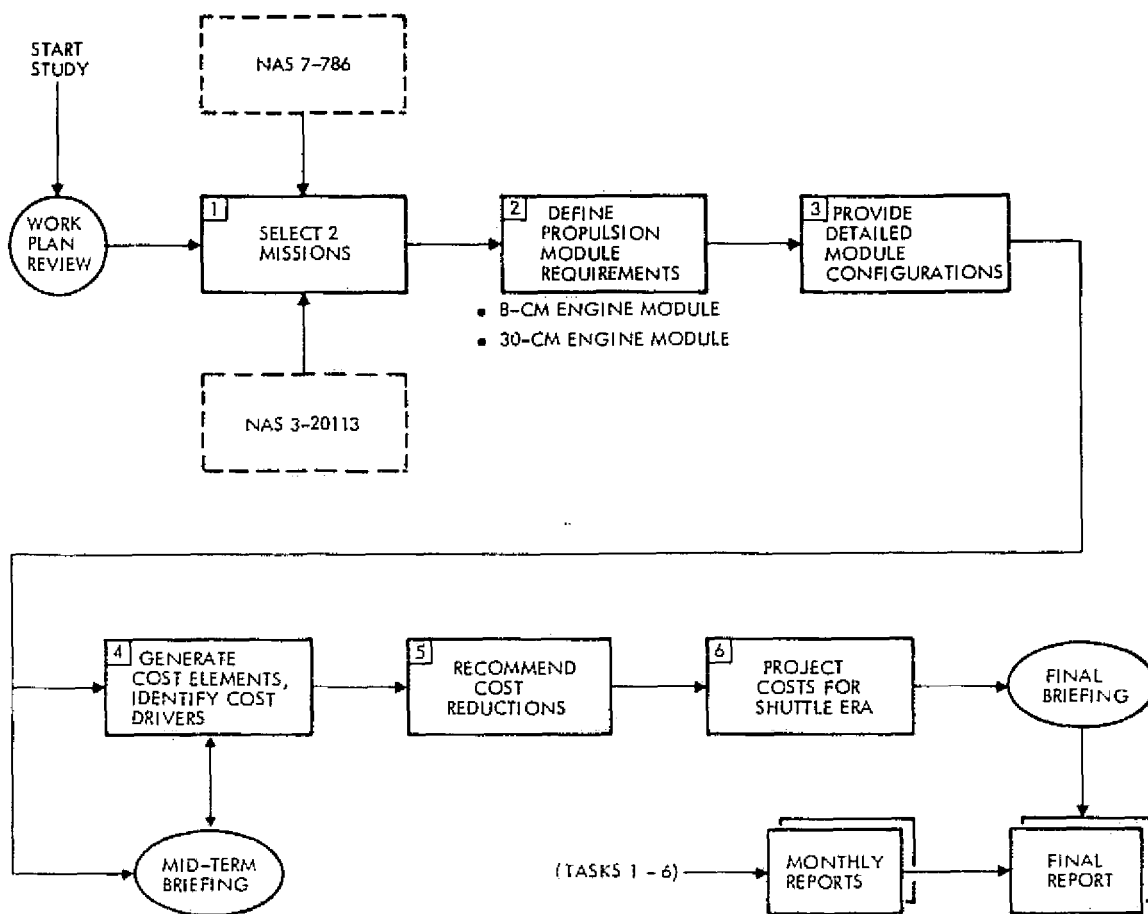


Figure 1. Ion Propulsion Cost Effectivity Study Activity Flow Diagram

and geosynchronous orbit stationkeeping. The other mission selected is for sun-synchronous satellite servicing.

The MMS is the standardized spacecraft bus which is intended for a range of missions in the Space Shuttle era. It is described in detail in Reference 3. New projects can be adapted to the capabilities of the MMS without going through a costly spacecraft design and development effort. NASA-GSFC is the technical manager for the MMS.

The MMS bus, shown in Figure 2, is composed of a module support structure with major modules for (1) communications and data handling (C&DH), (2) electric power, and (3) attitude control. In addition, there are adapter structures to attach to the payload and launch vehicle and a standard Tracking and Data Relay Satellite System (TDRSS) antenna. An

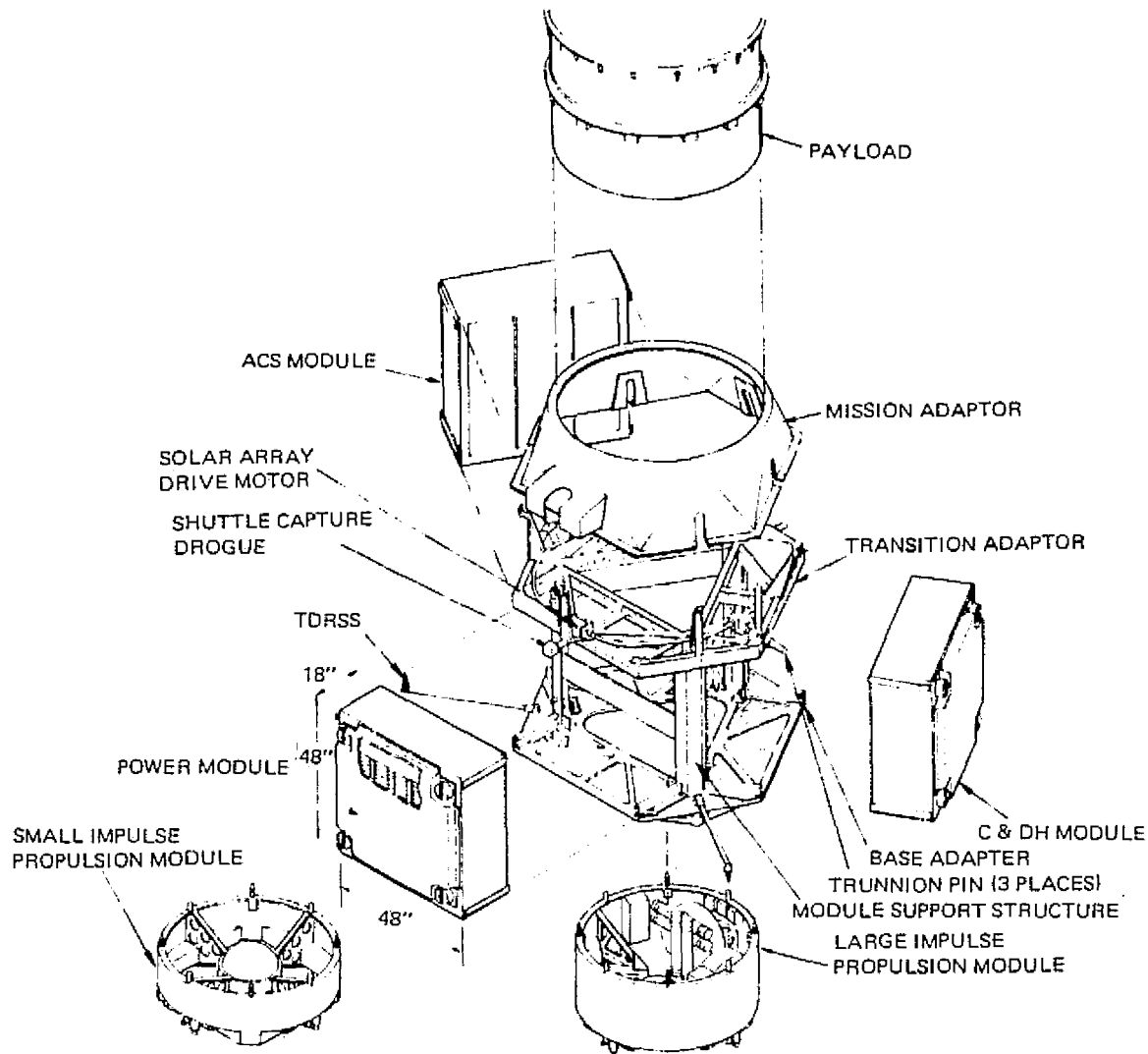


Figure 2. Multimission Modular Spacecraft Bus (exploded view)

optional propulsion module is used as required by the user mission. There are mission-unique subsystem elements which can be added to each module, such as a tape recorder or additional batteries. Antennas and solar arrays are considered to be mission-unique.

There are two propulsion/actuation modules now included in the standard MMS equipment list. Both use monopropellant hydrazine. The basic small impulse spacecraft propulsion subsystem (SPS-I) is sized to provide orbit adjust and reaction control for a typical spacecraft mission. SPS-I is expanded to the large impulse SPS-II for missions that require

orbit transfer or north-south stationkeeping. SPS-II uses the same rocket engine modules as SPS-I, but has a larger propellant tank and two additional thrusters for orbit transfer. A high-performance propulsion module, using ion engines, would be smaller and much lighter than the hydrazine system for most of the SPS-II applications.

The HPPM mission is described in Section 2 of this report. The mission for sun-synchronous satellite servicing is described in Section 3.

## 2. HIGH PERFORMANCE PROPULSION MODULE

Two potential MMS payloads have been studied to examine the use and advantages of 8-cm mercury ion thrusters in an HPPM. These are (1) a geosynchronous mission with tight pointing accuracy requirements, represented by StormSat (NASA Payload EO-15-A), and (2) a low earth orbit mission with significant orbital maneuvers or drag makeup, represented by an advanced LandSat (NASA Payload EO-08-A). The mission descriptions and ground rules used (in Reference 2) to design the HPPM are shown in Table 1.

The HPPM is primarily used on the MMS for orbital corrections, such as stationkeeping or orbit change, where a large added velocity ( $\Delta v$ )

Table 1. HPPM Missions on MMS

Description	MMS Geosynchronous Orbit Mission (e.g., StormSat)	MMS Low Earth Orbit Mission (e.g., LandSat)
Payoffs with ion propulsion	<ul style="list-style-type: none"> <li>• More payload mass</li> <li>• Lower launch costs</li> </ul>	<ul style="list-style-type: none"> <li>• More payload mass</li> <li>• Lower launch costs</li> <li>• Increased lifetime</li> </ul>
Orbit	Geosynchronous	705 to 914 km
Spacecraft mass (beginning of life)	1000 kg (assumed)	1700 kg
Mission life	3 yr	2 yr
Total north-south station-keeping $\Delta v$ requirement	150 m/sec	217 m/sec*
North-south stationkeeping	$\pm 0.1$ deg	---
Spacecraft ACS mode	3 reaction wheels plus propulsion	3 reaction wheels plus propulsion
Control functions	<ul style="list-style-type: none"> <li>• Acquisition</li> <li>• N-S and E-W stationkeeping</li> <li>• Momentum dump</li> <li>• Safehold backup mode</li> </ul>	<ul style="list-style-type: none"> <li>• Acquisition</li> <li>• Drag makeup and maneuvers</li> <li>• Momentum dump</li> <li>• Safehold backup mode</li> </ul>
Spacecraft power load	400 to 600 watts	<ul style="list-style-type: none"> <li>• 261.8 watts minimum for 93 minutes</li> <li>• 450 watts average</li> <li>• 2200 watts peak for 10 minutes</li> </ul>
Pointing accuracy	<ul style="list-style-type: none"> <li>• <math>10^{-2}</math> deg accuracy</li> <li>• <math>10^{-6}</math> deg/sec drift rate deviation</li> <li>• <math>6 \times 10^{-4}</math> deg attitude jitter</li> <li>• Safehold peak error of 10 deg</li> </ul>	
Bus voltage	28 $\pm$ 7 volts	
Spacecraft power sources	<ul style="list-style-type: none"> <li>• Hybrid solar cells</li> <li>• Lightweight nickel-cadmium batteries</li> </ul>	
*for orbital maneuvers		

is required. Ion propulsion also becomes an attractive vehicle for unloading wheel momentum and can be used for auxiliary control functions, such as acquisition and failure mode operation.

The fine level of control possible with ion propulsion permits it to be a backup to the reaction wheels for control of satellite pointing during an experiment. The ability of ion propulsion to provide stationkeeping or orbit sustenance with very low disturbances may be more significant than the weight savings resulting from the high specific impulse.

## 2.1 GEOSYNCHRONOUS ORBIT MMS MISSION

A representative MMS StormSat configuration using the high-performance propulsion module with ion engines is shown in Figure 3. The ion thrusters are oriented so that each thrust vector nominally points through the spacecraft center of mass. The pairs are symmetrically inclined with respect to the north-south axis by 15 to 30 degrees, depending on the spacecraft disturbance torque levels. The thrusters are oriented to point nominally through the center of mass, with a small cant angle to

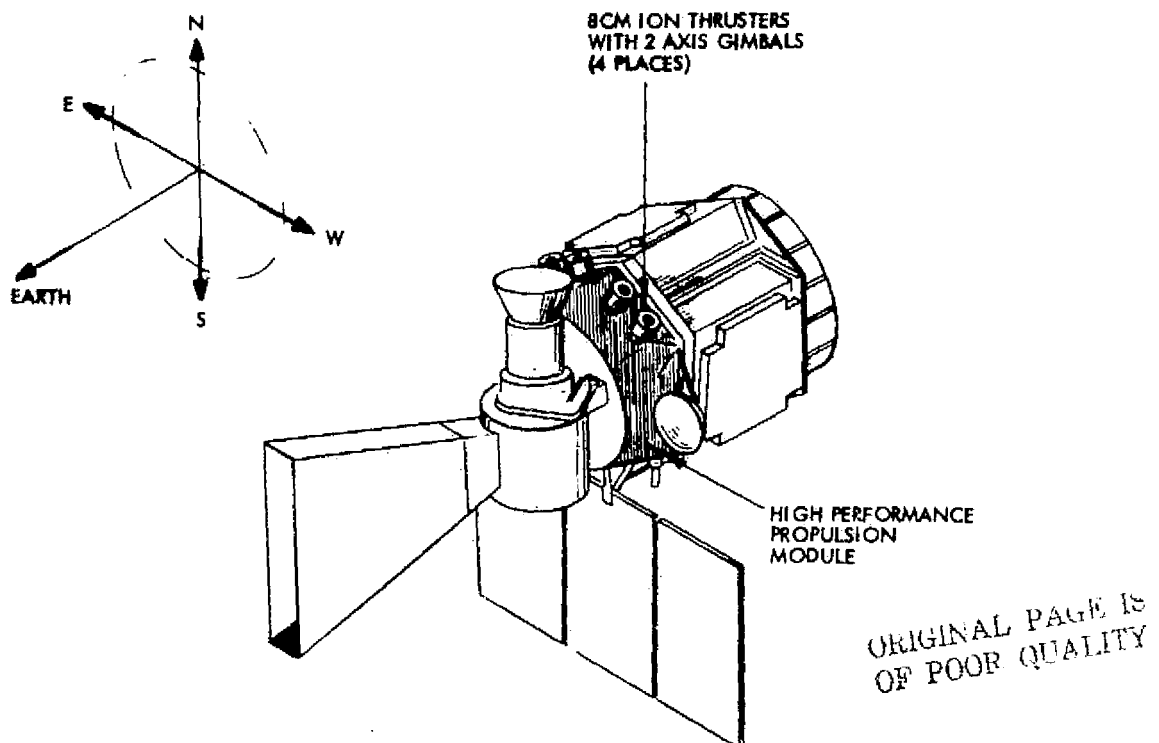


Figure 3. MMS StormSat Configuration with the HPPM

offset the solar pressure torques acting on the large solar array panel. The ion engines permit dumping of large amounts of momentum with very small propellant penalty. The various modes that ion propulsion may be used for on the geosynchronous MMS missions are discussed below. Note that the spacecraft is assumed to be orbited by the Space Shuttle and has no transfer orbit attitude control requirements.

#### 2.1.1 Acquisition and Reacquisition

Acquisition with MMS is more efficient than with typical geosynchronous communications satellites because of three factors: (1) the tip-off rates from a Shuttle launch are smaller than the residual body rates due to despin experienced with an expendable launch vehicle, (2) the spacecraft moments of inertia are lower, and (3) the MMS attitude control subsystem (ACS) is more sophisticated, with the equivalent of an inertial platform and elaborate computer-programmed search algorithms.

Acquisition with ion propulsion can be accomplished within several hours. Even though this is longer than is possible with hydrazine, it is acceptable. Two gimballed thrusters are fired to provide sources of controllable torque.

#### 2.1.2 Stationkeeping

On the geosynchronous MMS, north or south and east or west stationkeeping is performed only once per day, except when eclipse interferes with the operation. Two opposing thrusters are fired for north or south velocity increments (depending on satellite orientation). East or west velocity increments are achieved by turning off the west or east thruster near the end of a stationkeeping period. The thrusters fire approximately 5.3 hours per day. Firing starts with the thrusters vectored in a direction to minimize start-up torques.

For this mission, ion propulsion shows considerable advantage over hydrazine. The start-up transients from thruster misalignment are much smaller because of the lower thrust level and ability to produce very small torques. This advantage permits the consideration of performing experiments even during the stationkeeping maneuvers and maintaining the required attitude control.



### 2.1.3 Momentum Dump

After the stationkeeping maneuver has started, the ion thrusters are gradually rotated in a direction which permits momentum wheel unloading. MMS currently is designed to use magnetic torquers or hydrazine thrusters to unload momentum. These are both unattractive for this application since the earth's magnetic field is undependable at geosynchronous orbit and hydrazine thrusters can cause unacceptable attitude transients.

## 2.2 LOW EARTH ORBIT MMS MISSION

This class is representative of those scientific missions (earth pointing, or otherwise) which require an orbit altitude of 425 to 1850 km (230 to 1000 nmi) with precisely controlled orbital parameters. Figure 4 shows a possible MMS configuration for this class of missions. Aerodynamic drag will cause the orbit to decay, especially at the lower end of the altitude range. Generally, orbital sustenance is not essential for mission completion, but it can simplify sensor data processing and may be highly desirable.

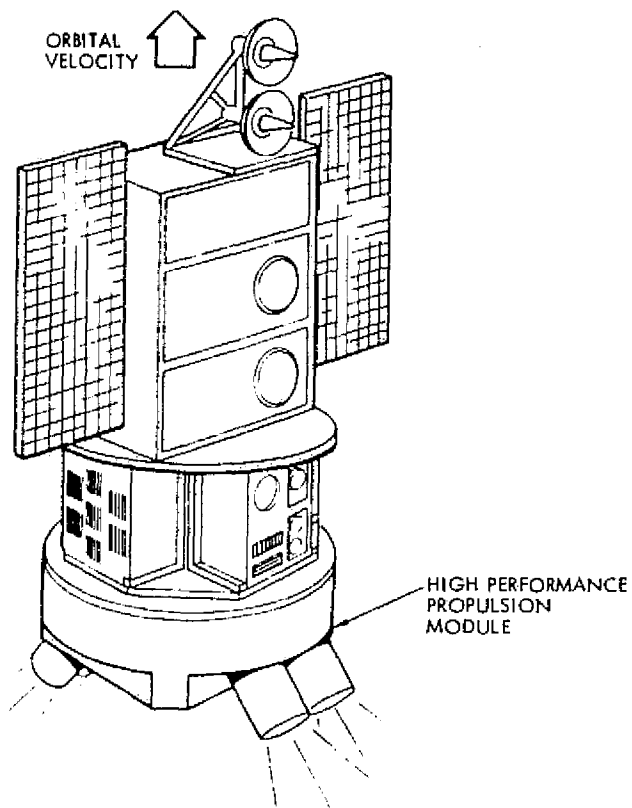


Figure 4. Possible Low Earth Orbit MMS Mission with the HPPM

As with the geosynchronous mission, extremely tight experiment pointing is required. The attitude control subsystem module is identical to the one used for the geosynchronous MMS. The propulsion subsystem is required to cycle much more frequently at this altitude because of the need for unloading the accumulated momentum of the wheels that the gravity gradient and aerodynamic disturbance torques create. The thrusters are fired in pairs to produce a velocity increment along the bisecting line of the two thrusters and are differentially gimballed to produce the desired attitude control torques.

Acquisition and momentum dump for this mission are accomplished identically to the geosynchronous cases. The main function of the thrusters in low earth orbit is to achieve orbital control. This can be drag make-up or maneuvers to change orbits. The engines are intended to be fired continuously (or as continuously as possible) to achieve the desired velocity increment. The thrusters are symmetrically canted toward the bisecting vector or away from it to achieve the desired steady state acceleration. In this manner, a large range of steady state thrust levels can be achieved.

Continuous thrusting is desired because (1) this maintains high propellant efficiency since the weight penalty of continuous versus intermittent thrusting is small, (2) the 2-year mission life is easily met, (3) momentum dumping is continuously available, and (4) the number of thruster cycles is reduced. Momentum accumulation in low earth orbits is rapid due to the increased influences of gravity gradient, aerodynamic and magnetic disturbances.

### 2.3 CONFIGURATION

The propulsion subsystem schematic for the HPPM is shown in Figure 5. The subsystem incorporates four 8-cm mercury ion thrusters and their associated equipment. The equipment complement for each thruster is described in Reference 4 except that the previous digital interface unit (DIU) and digital control unit (DCU) have been replaced by a single controller and interface unit (DCIU), following the approach taken in Reference 5. Thus, the electrical power processing equipment consists of a power electronics unit (PEU) and DCIU for each thruster and gimbal assembly. Two propellant reservoirs are required for the

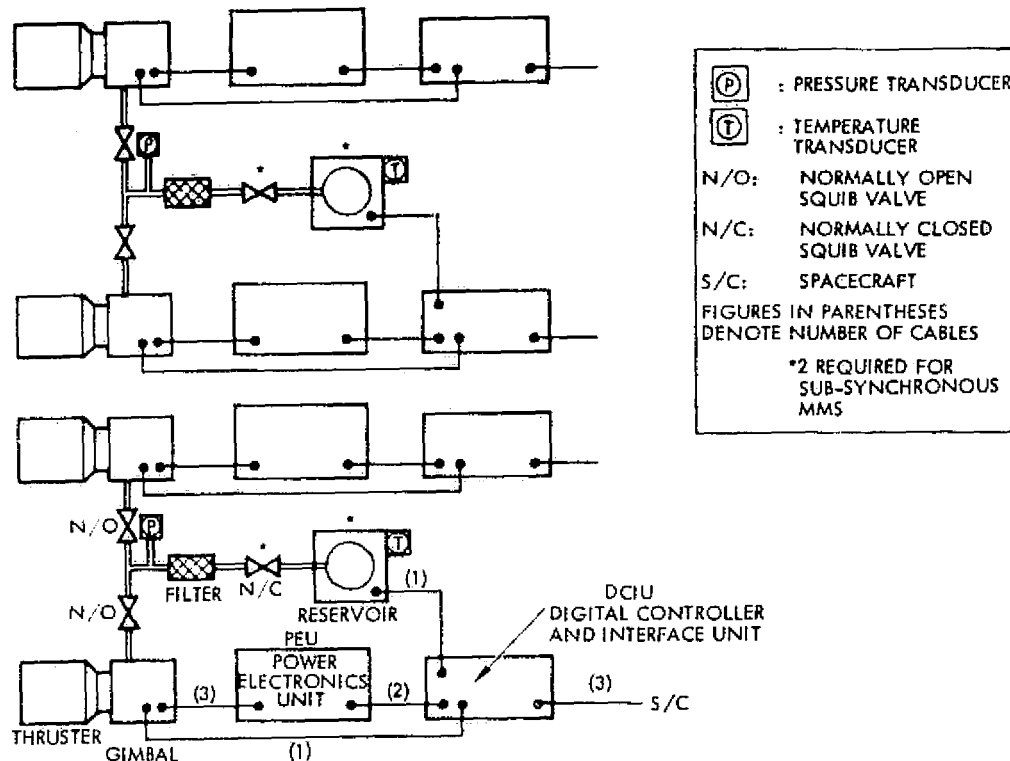


Figure 5. Baseline Propulsion Subsystem Schematic for HPPM

geosynchronous HPPM mission, and four are required for the low-earth orbit mission. The valves, filters, and transducers used with the propellant supply are identified on the schematic diagram.

### 2.3.1 8-cm Ion Thruster Power Processor

The 8-cm ion engine power processing equipment is presently in the engineering model phase (Reference 6) and is planned for launch in 1981 on an Air Force satellite. The flight test (Reference 5) is designated as SAMSO-601 and will be flown aboard the Shuttle-launched Air Force Space Test Program P80-1 satellite.

Figure 6 shows the major functions in the power processor. The main input power is  $70 \pm 20$  Vdc power bus. The original power processor was being developed for the 5-cm ion engine for the CTS satellite which had the unregulated 70-volt solar array bus. The HPPM application of the 8-cm ion engine will be with a spacecraft bus voltage of  $28 \pm 5$  Vdc. Provision must be provided to make the spacecraft voltage compatible with the design input power voltage of the 8 cm power processor.

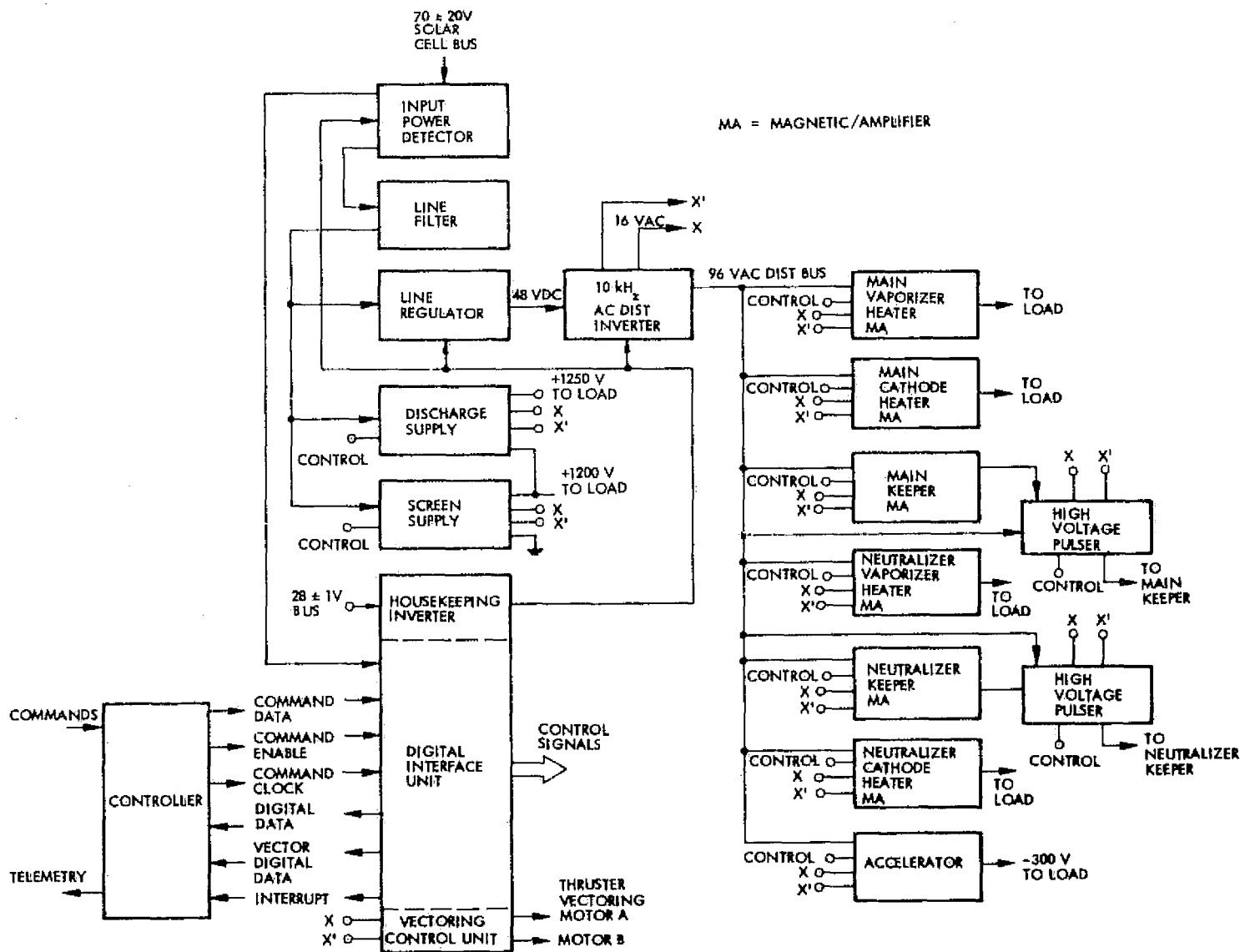


Figure 6. Power Processor Functional Block Diagram

ORIGINAL PAGE IS  
OF POOR QUALITY

The dc power is monitored by the input power detector and sends a command signal to the digital interface unit to shut down during abnormal operating modes.

The dc power is then fed to a line filter which alternates the switching currents generated by the different pulse width regulators. DC power is fed to the following power electronics:

- 48 Vdc line regulator
- Discharge supply
- Screen supply

The regulated 48 Vdc bus goes through a 10 kHz dc to ac inverter which supplies power to the following ion engine components:

- Main vaporizer heater
- Main cathode heater
- Main keeper and high voltage pulser
- Neutralizer vaporizer heater
- Neutralizer keeper and high voltage pulser
- Neutralizer cathode heater
- Accelerator

A 28-volt  $\pm 1$  Vdc bus provides power to all of the low level electronics.

The digital interface unit accepts a serial data command and provides parallel data lines to turn the power supplies on and off, to command the set points for each power supply and to encode internal power processor telemetry data for transfer back to a central computer. Seventy-four discrete on/off and set points, and 128 step commands each for the neutralizer keeper current, discharge current, and discharge voltage are provided. Twenty-one telemetry measurements are used to monitor ion thruster operation.

Reference 5 states that the digital interface unit is being modified to include a microprocessor which will control the complete ion engine operation, such as start-up, run, and recycle after ion engine arcs. The microprocessor will eliminate the need for the central spacecraft computer to monitor and control the operation of the thrust subsystem.

The power processor employs three separate grounds. These are:

- Frame (ion engine output ground)
- Command return ground
- Unit common for internal control electronics

All power circuit isolation is provided by magnetic transformer isolation. The control electronic power is isolated by the transformer in the house-keeping inverter and the magnetic current control and sensing windings. The command lines are isolated by optical couplers.

The baseline HPPM power processor will not require as many power processing functions as are contained in the engineering model. It only retains those features that are representative of spaceflight operational use, and omits features better suited for flight diagnostics.

The baseline power processor is divided into two mechanical assemblies: the power electronics unit (PEU), and the DCIU. For the MMS applications studied, the baseline PEU remains the same as described in Reference 4. The DCIU, however, now becomes a simplified command and protection unit. Table 2 lists the command and telemetry requirements that are consistent with a flight thruster subsystem configuration. All commands are discrete pulses and all telemetry signals are 0 to 5 Vdc analog functions. The commands have optical isolation and the telemetry has magnetic isolation to protect against ground current between the power processor and the data handling subsystem.

Table 2. Command and Telemetry List

<u>Commands</u>	(Pulse Commands)
Idle (Preheat)	
On	
Off	
<u>Telemetry</u>	(Analog Signals)
Beam Current	
Beam Voltage	
Neutralizer Emission Current	
Accelerator Current	

Baseline power processor characteristics for both the PEU and DCIU are presented in Table 3, where they are also compared with the engineering model. Tables 4 and 5 show the detailed function part count for these units. Table 5 is derived from the information contained in Reference 7, and reflects the elimination of digital interface functions and vectoring electronics from the previous DIU. Compared to the 530 parts in the baseline DCIU, the DIU analyzed in Reference 7 contains 935 parts, and the DCU identified in Reference 2 has 20 parts (955 parts total).

The total part count for each baseline 8-cm thruster power processor is 1419 parts.

### 2.3.2 HPPM Performance and Interface Requirements

The HPPM meets all the interface requirements for any MMS propulsion actuation module (Reference 3). As shown in Figure 7, it is cylindrical and can be mounted at the "bottom" end of the MMS. Specific design features of the HPPM are listed in the figure. Details for a low-earth orbit configuration are shown in the layout drawing, Figure 8.

The module contains four thrusters, which are fired in pairs or alone. Two thrusters are fired together at one node per day for north-south stationkeeping or continuously for orbit sustenance or orbit maneuvers. They are gimballed and time-phased for attitude control and other maneuvers. The other pair are in standby redundancy; either pair can drain the propellant reservoirs.

The module in this form has enough propellant for two engines to thrust for 20,000 hours each. This is more than enough total impulse to satisfy the two missions considered. Table 6 summarizes the significant ion thruster performance requirements for these missions. Propellant can be off-loaded for missions with lesser requirements.

Thermal control for the propulsion subsystem is a localized integration task because the subsystem is completely contained within the propulsion actuation module. Therefore, thermal control is handled with the subsystem's thermal control features.

Table 3. Power Processor Unit Characteristics for 8-cm Ion Thruster

	ENGINEERING MODEL	BASELINE
POWER ELECTRONICS UNIT (PEU)		
MASS, KG (LB)		7.0 (15.4)
INPUT VOLTAGE, VDC		70 ± 20
INPUT POWER, WATTS		160
POWER CONVERSION EFFICIENCY, %		74.5
SIZE, INCHES (CM)		4.3 × 7.9 × 15.2 (10.9 × 20.1 × 38.6)
PART COUNT		889
DIGITAL CONTROLLER AND INTERFACE UNIT (DCIU)	DCU*	DIU
MASS, KG (LB)	2.3 (5.0)	3.2 (7.0)
INPUT VOLTAGE, VDC	28 ± 1	28 ± 1
INPUT POWER, WATTS	3	5
SIZE, INCHES (CM)	---	4.3 × 7.9 × 7.9 9 (10.9 × 20.1 × 20.1)
PART COUNT	20	935
TOTAL PART COUNT	955	530
POWER PROCESSOR PART COUNT	1844	1419

\* DIGITAL CONTROL UNIT PER REFERENCE 4. NOT DEVELOPED AS PART OF ENGINEERING MODEL.

Table 4. Power Electronics Unit Part Count Analysis (Reference 7)

Function	Part Count
Main vaporizer heater	40
Neutralizer vaporizer heater	40
Main cathode heater	49
Neutralizer cathode heater	49
Neutralizer keeper	81
Main keeper	87
Line regulator	58
10 kHz distributor inverter	25
Screen supply	152
Main high voltage pulser	22
Neutralizer high voltage pulser	22
Discharge supply	115
Line filter	19
Accelerator	130
Total	889



Table 5. Digital Controller and Interface Unit Part Count Analysis

Function	Part Count
Power supply and filters	107
Neutralizer vaporizer heater control	8
Discharge current reference	9
Main vaporizer current reference	9
Supplies on/off and discharge on command registers	6
Neutralizer vaporizer heater setpoint	1
Neutralizer heater setpoint	28
Interrupt and accelerator current high register	2
Neutralizer keeper setpoints	15
Cathode vaporizer heater setpoints	18
Cathode heater setpoints	19
Cathode keeper setpoints	15
Thruster vector enable	4
Main keeper high voltage on	9
Neutralizer keeper high voltage on	9
Main keeper current < constant A	9
Neutralizer keeper current < constant B	9
Beam current < constant C	9
Beam current > constant D	9
Accelerator current > constant E	9
Frequency generator	6
Recycle timing circuitry	11
Main vaporizer heater control loop amplifier	19
Neutralizer vaporizer heater control loop amplifier	14
Discharge output and ramp circuitry	26
Inhibit output circuitry	14
16-volt inhibit optical isolator	5
Screen command optical isolator	5
Accelerator command optical isolator	5
Undervoltage sensor	11
High power sensor	57
Housekeeping inverter	55
Total	530

ORIGINAL PAGE  
OF POOR QUALITY

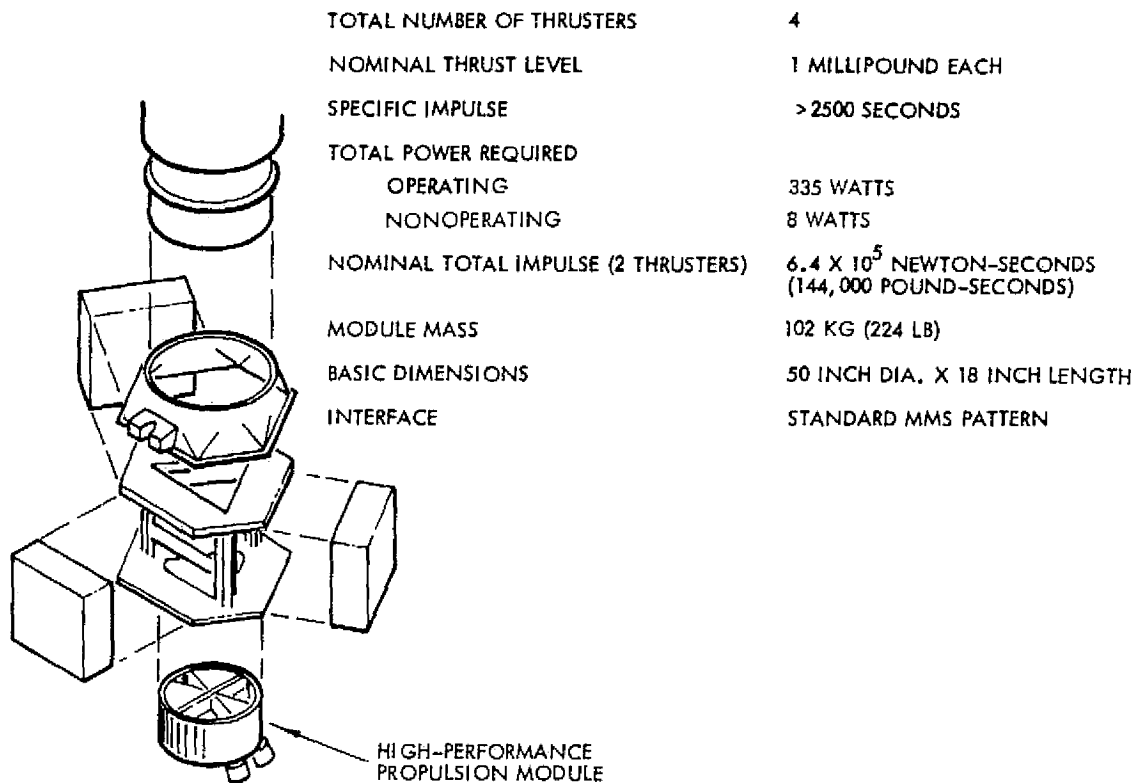


Figure 7. High Performance Propulsion Module for MMS

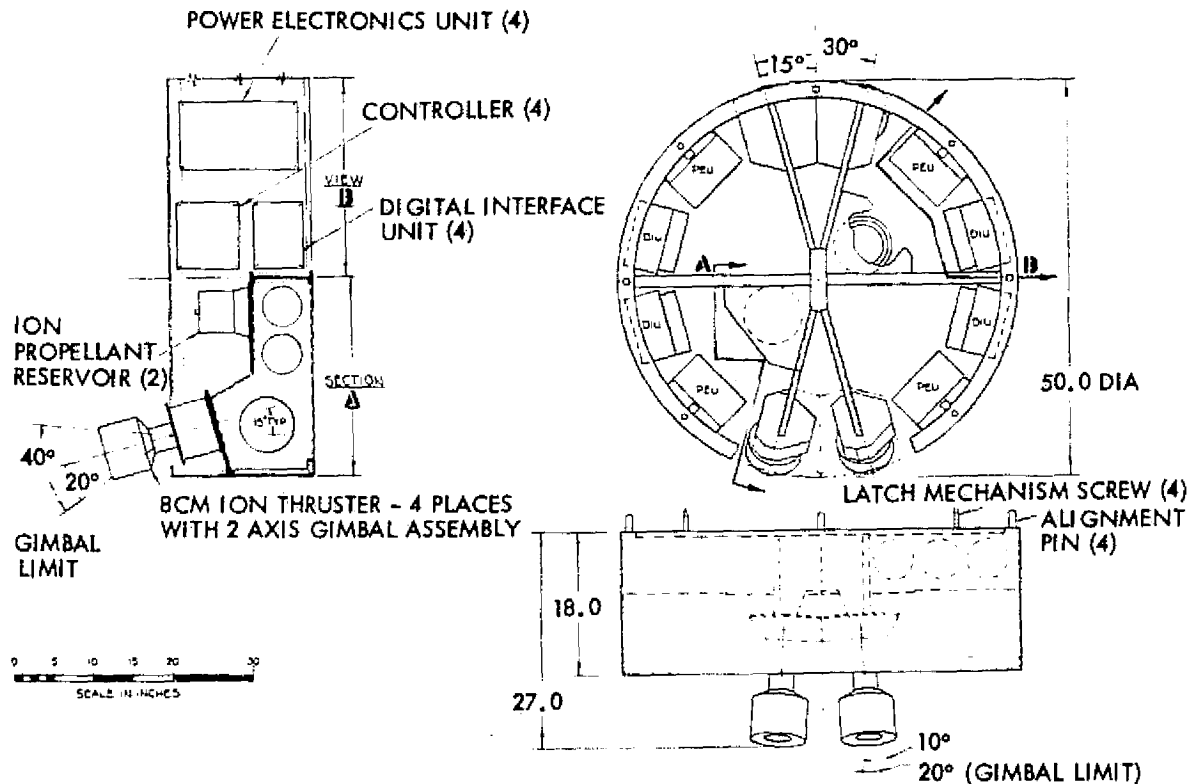


Figure 8. Layout of High Performance Propulsion Module with Low Earth Orbit Mission Configuration

Table 6. Ion Thruster Performance Requirements for MMS Missions

	Station Acquisition	N-S, E-W Stationkeeping	Orbit Maneuvers	Momentum Dump	Total
<u>Geosynchronous MMS*</u>					
Number of cycles (total)	1	1,095	--	Included	1,095
Worst thruster	1	1,095	--	Included	1,095
Hours used (total)	.6	5,913	--	Included	5,914
Worst thruster	.6	5,913	--	Included	5,914
Propellant used (kg)	<.1	6.8	--	--	6.8
<u>Low Earth Orbit MMS**</u>					
Number of cycles (total)	1	--	1 to 10	Included	2 to 11
Worst thruster	1	--	1 to 10	Included	2 to 11
Hours used (total)	.6	--	17,520	Included	17,521
Worst thruster	.6	--	17,520	Included	17,521
Propellant used (kg)	<.1	--	24.3	--	24.3
*3-year mission. Stationkeeping values shown scale linearly with time.					
**2-year mission. Propellant usage calculated for worst case where thrusting is continuous.					

Several factors have been considered to ensure that the HPPM is compatible with the Shuttle:

- No single point failure will prevent retrieval of the spacecraft by the Shuttle. The spacecraft will go into a passive safhold mode which will allow retrieval.
- The propulsion module can be disconnected on orbit for servicing. The MMS is designed for on-orbit servicing and the complete propulsion module can be interchanged.
- The only module interface is with the rest of the spacecraft. There is no active tie to the Shuttle orbiter or an upper stage. The module structure may be used as a structural load path, but this is a simple interface.
- There will be no mercury contamination of the Shuttle orbiter payload bay. The vaporizer and valves are designed so that two failures would have to occur before there would be spillage into the bay.
- The HPPM is compatible with the Shuttle environment. Environmental data on the Shuttle orbiter and/or upper stage will be used for detailed design.

The short 18-inch (0.46 meter) length of the HPPM is a very attractive feature. This compares with 5 feet (1.5 meters) for the standard SPS-II hydrazine propulsion module (Reference 8). The pricing policy for Shuttle-launched spacecraft puts a premium on shorter-length designs.

### 2.3.3 Propulsion Subsystem Weight

The ion propulsion subsystem dry weights for the geosynchronous and low earth orbit MMS missions are shown in Tables 7 and 8, respectively. The basic difference is that the low earth orbit configuration is sized to allow two engines to fire up to 20,000 hours each. This requires four reservoirs. Only two reservoirs, plus reduced lengths of lines and cables, are required for the geosynchronous mission.

### 2.3.4 Propulsion Subsystem Electrical Interface

The electrical interfaces between the propulsion subsystem and the MMS are presented in Table 9. The power subsystem interface is discussed in more detail in the next subsection. The interface with the command and data handling subsystem is straightforward and requires no further comment.

Table 7. Ion Propulsion Subsystem Weight, Geosynchronous MMS Mission

Hardware	Unit Mass (kg)	No. Required	Mass (kg)	Weight (lbm)
Thruster and gimbal assembly	3.7	4	14.8	32.6
Reservoir (a)	1.2	2	2.4	5.3
Power electronics unit	7.0	4	28.0	61.7
Digital controller and interface unit	2.6	4	10.4	22.9
Squib valve	0.1	6	0.6	1.3
Filter	0.1	2	0.2	0.4
Propellant lines	-	2	(b)	-
Cables	-	38	2.8	6.2
Total Dry Weight			59.2	130.4

(a) Includes pressurant, fill valves, pressure sensor, temperature sensor

(b) Less than 0.1 kg

Table 8. Ion Propulsion Subsystem Weight, Low Earth Orbit MMS Mission

Hardware	Unit Mass (kg)	No. Required	Mass (kg)	Weight (lbm)
Thruster and gimbal assembly	3.7	4	14.8	32.6
Reservoir (a)	1.2	4	4.8	10.6
Power electronics unit	7.0	4	28.0	61.7
Digital controller and interface unit	2.6	4	10.4	22.9
Squib valve	0.1	8	0.8	1.8
Filter	0.1	2	0.2	0.4
Propellant lines	-	2	(b)	-
Cables	-	40	2.8	6.2
Total Dry Weight			61.8	136.2

(a) Includes pressurant, fill valves, pressure sensor, temperature sensor

(b) Less than 0.1 kg

Table 9. Ion Propulsion Subsystem Electrical Interfaces for the HPPM

POWER	320 WATTS AT 70 ± 20 VDC 8 WATTS AT 28 ± 1 VDC 7 WATTS AT 28 VDC FOR EACH GIMBAL MOTOR ACTUATION			
COMMANDS	FUNCTION	TYPE	NO. REQ'D. (A) (B)	
	THRUSTER IDLE	DISCRETE	4	4
	THRUSTER ON	DISCRETE	4	4
	THRUST OFF	DISCRETE	4	4
	GIMBAL " +	DISCRETE	4	4
	GIMBAL " -	DISCRETE	4	4
	GIMBAL " +	DISCRETE	4	4
	GIMBAL " -	DISCRETE	4	4
	RESERVOIR VALVE	DISCRETE	2	4
	THRUSTER VALVE	DISCRETE	4	4
	TOTAL		34	36
TELEMETRY	SIGNAL	TYPE	NO. REQ'D. (A) (B)	
	BEAM CURRENT	ANALOG	4	4
	BEAM VOLTAGE	ANALOG	4	4
	NEUTRALIZER EMISSION CURRENT	ANALOG	4	4
	ACCELERATOR CURRENT	ANALOG	4	4
	RESERVOIR PRESSURE	ANALOG	2	4
	RESERVOIR TEMPERATURE	ANALOG	2	4
	TOTAL		20	24

(A) GEOSYNCHRONOUS MISSION

(B) LOW-EARTH ORBIT MISSION

ORIGINAL PAGE  
OF POOR QUALITY

### 2.3.5 Power Subsystem Configuration

Two power sources are required for the 8-cm thruster power processor. These are:

- 1)  $70 \pm 20$  Vdc for the main thruster operation
- 2)  $28 \pm 1$  Vdc of auxiliary power

In order to make the power subsystem compatible with these requirements, a boost line regulator design option was selected (Reference 2). Figure 9 presents the electric power subsystem diagram for this option, where the standard MMS power bus is used for the electric propulsion subsystem. DC-DC boost regulators are used to step up the standard 28 Vdc bus to a 55-volt bus at the ion engine power processor. To optimize the ion engine power processor efficiency, 55 volts was chosen since the power processor is capable of operation between 50- and 90-volt inputs. The 55-volt output also reduces the weight of the boost regulator. A redundant dc-dc converter is used to provide regulated 28-volt power to the power processor.

HPPM interactions with the MMS power module were analyzed in Reference 2. From this analysis, additional solar array and battery increments were added to the spacecraft power source to accommodate the propulsion module. The baseline electrical interface (Table 9) differs

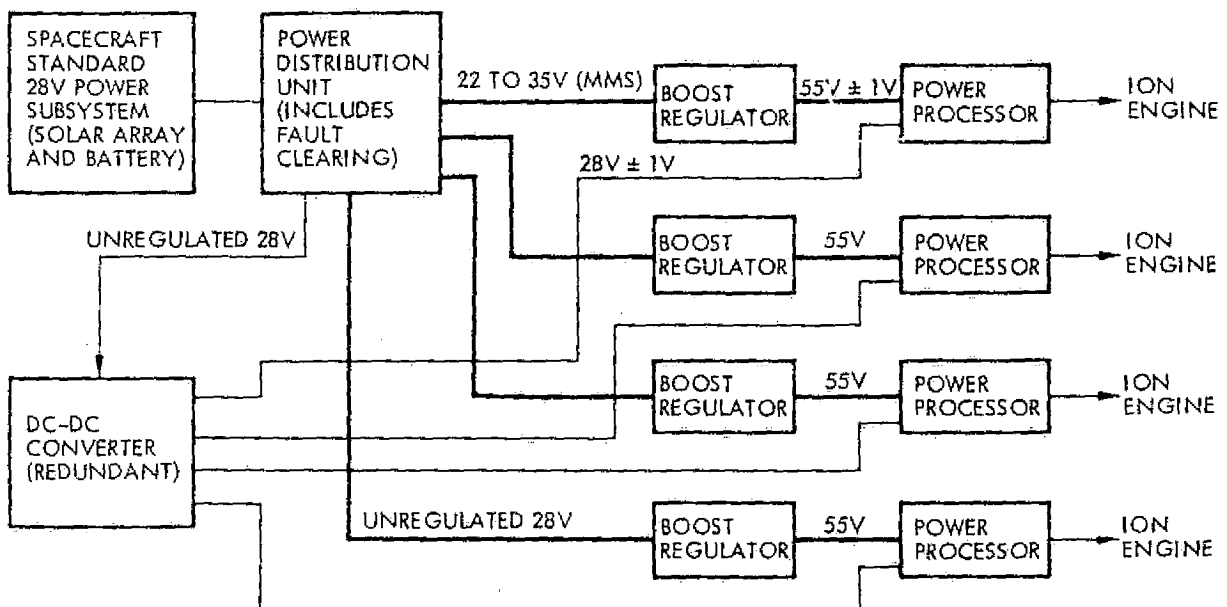


Figure 9. Electric Power Distribution to HPPM Ion Engines

slightly from the interface previously studied, in that the baseline requires slightly less power. The impact, if any, of this small difference is insignificant. Thus, the results from the previous analysis are used.

### 2.3.6 Net Weight Impact

The net weight impact of the HPPM on the MMS is shown in Table 10. Propulsion subsystem dry weight data are presented in Section 2.3.3. Propellant requirements were summarized in Table 6. The power subsystem weight impact, for the boost line regulators, dc-dc converters, and additional solar array and battery requirements, are taken from Reference 2, as is the weight estimate for the module structure.

For comparison, a hydrazine SPS-II propulsion module having the same total impulse capability as the HPPM would weigh 430 kg (947 pounds). Thus, the HPPM makes 264 kg (580 pounds) available for added payload.

For the geosynchronous MMS mission only, a hydrazine SPS-I propulsion module weighing 158 kg (347 pounds) could be used. By going to the HPPM, an additional 71 kg (154 pounds) would be available for payload.

Table 10. Net Weight Impact of High Performance Propulsion Module on MMS

ITEM	GEOSYNCHRONOUS MISSION		LOW EARTH ORBIT MISSION	
	KG	LB	KG	LB
ION PROPULSION SUBSYSTEM	59.2	130.4	61.8	136.2
PROPELLANT	6.8	15.0	24.3	53.5
BOOST LINE REGULATORS AND DC-DC CONVERTERS	7.3	16.0	7.3	16.0
MODULE STRUCTURE	8.3	18.3	8.3	18.3
ADDITIONAL SOLAR ARRAY	5.8*	12.8	28.6	63.0
ADDITIONAL BATTERY	----	-----	36.1	79.5
TOTAL	87.4	192.5	166.4	366.5
*ASSUMES 600-WATT SPACECRAFT LOAD ARRAY				

## 2.4 COST ELEMENTS

Cost estimates were generated for the baseline HPPM in both its synchronous and low earth orbit configurations. All cost estimates are presented in 1978 dollars.

Table 11 lists recurring and nonrecurring cost estimates for the HPPM in its geosynchronous mission configuration. Similarly, Table 12 contains estimates for the HPPM in its low earth orbit configuration. Start-up costs have been excluded from the estimates shown. It was assumed that similar hardware would be in production at the time that the subsystem was needed for application.

Nonrecurring costs assume a 2-1/2 year time span for development and qualification. Environmental and electromagnetic compatibility (EMC) tests are performed at the subsystem component level (thruster, PEU, etc.) and at the spacecraft system level. By virtue of HPPM symmetry, only one propulsion half-system is required for development and another propulsion half-system for qualification. Development testing at the subsystem level includes thermal-vacuum and thrusters/power processors integration tests. Qualification testing at the subsystem level includes thermal-vacuum and mission duty cycle tests. The mission duty cycle is performed with a single thruster/power processor combination.

Cost estimates for the 8-cm thruster and propellant reservoir are based on NASA-Lewis Research Center (NASA-LeRC) experience with single unit purchases (Reference 9). Other fluid component estimates are based on TRW experience with similar hardware. Cost estimates for the power processor (PEU and DCIU) are based on detailed costing data generated for Reference 10, and on part count comparisons. Boost regulator and dc-dc converter estimates are based on TRW experience with power conversion electronics equipment. The estimates for structure, thermal control, integration and assembly costs are based on Rockwell International analysis of hydrazine propulsion module costs for MMS (Reference 11). The Rockwell estimates have been adjusted to 1978 dollars, and provision made for the added complexity of electronics integration. Solar array costs are based on Lockheed data for the Solar Electric Propulsion (SEP) array (Reference 12). The SEP array is being



Table 11. Baseline HPPM Cost Breakdown, Synchronous Mission

Item	Nonrecurring Costs (\$ millions)	Recurring		
		Unit Cost (\$ millions)	Quantity	Total (\$ millions)
Hardware				
Thruster and Gimbal Assembly	0.485	0.112	4 ea	0.448
Propellant Storage and Distribution	0.178	--	1 set	0.147
Power Electronics Unit	1.869	0.122	4 ea	0.488
Digital Controller and Interface Unit	1.223	0.076	4 ea	0.304
Structure and Thermal Control	0.309	--	As req'd	0.067
Integration and Assembly	0.348	--	As req'd	0.241
Boost Regulator	0.188	0.024	4 ea	0.096
DC-DC Converter	0.146	0.018	2 ea	0.036
Additional Solar Array	0.100	--	9.7 M <sup>2</sup>	0.220
Additional Battery	0.025	0.100	1 ea	0.100
Programmatic				
Aerospace Ground Equipment	0.734			0.007
Launch Operations	0.025			-0-
Development Tests	0.066			-0-
Qualification Tests	0.030			-0-
Subsystem Engineering	0.266			0.017
Reliability and Quality Assurance	0.084			0.150
Project Management	0.528			0.202
Total	6.604			2.523

Table 12. Baseline HPPM Cost Breakdown, Low Earth Orbit Mission

Item	Nonrecurring Costs (\$ millions)	Recurring		
		Unit Cost (\$ millions)	Quantity	Total (\$ millions)
Hardware				
Thruster and Gimbal Assembly	0.485	0.112	4 ea	0.448
Propellant Storage and Distribution	0.113	--	1 set	0.082
Power Electronics Unit	1.869	0.122	4 ea	0.488
Digital Controller and Interface Unit	1.223	0.076	4 ea	0.304
Structure and Thermal Control	0.309	--	As req'd	0.067
Integration and Assembly	0.310	--	As req'd	0.204
Boost Regulator	0.188	0.024	4 ea	0.096
DC-DC Converter	0.146	0.018	2 ea	0.036
Additional Solar Array	0.100	--	3 M <sup>2</sup>	0.053
Programmatic				
Aerospace Ground Equipment	0.734			0.007
Launch Operations	0.025			-0-
Development Tests	0.066			-0-
Qualification Tests	0.072			-0-
Subsystem Engineering	0.266			0.017
Reliability and Quality Assurance	0.080			0.124
Project Management	0.521			0.167
Total	6.507			2.093

developed by Lockheed under the management of NASA-Marshall Space Flight Center. The battery cost estimate is based on the use of a NASA standard unit added to the MMS power module.

Aerospace ground equipment (AGE) for the HPPM primarily consists of power processor, boost regulator, dc-dc converter test equipment, input controllers for the power processor, and ion engine load simulators. Subsystem engineering, reliability, and quality assurance costs listed under programmatic costs comprise those costs not included previously under component engineering and product assurance. Subsystem quality assurance costs were derived parametrically, and were calculated as 7% of total hardware costs, excluding the solar array. Project management was similarly derived parametrically, and was taken as 8% of total project cost.

#### 2.4.1 Hardware Cost Factors

Examination of Tables 11 and 12 shows that the largest hardware cost elements are in the power processor and the thruster.

The reasons why ion propulsion power processing costs are so high are related to the relatively high part count and the fact that many of these parts are handling relatively high power levels. Elaborate machining is employed in the construction of the power processing units to minimize structural weight while maintaining component temperature control. Special assembly and inspection procedures are implemented to assure good thermal contact between parts and structure during operation. Magnetics fabrication for the power processor requires special assembly and potting procedures to assure low internal corona levels, and in-process screening tests at high voltage under vacuum conditions to verify component integrity.

Refractory materials are used in construction of the ion thruster, which add both to machining and assembly costs. High perveance (small dimension) electrode pairs are employed to obtain the desired performance characteristics. Dished grid optics are needed to avoid electrical shorts between electrodes from thermal gradients. The engine discharge chamber interior surfaces are specially treated to minimize internal sputtering effects. Insulators in the thruster contain sputter shields for protection

from coating over with sputtered films. Hollow cathodes are used for electron sources, both in the discharge and the neutralizer. These cathodes contain specially impregnated inserts, and operate with thermionic electron emission control. Additionally, the vaporizer flow restrictions contain porous plugs, which require pore size control for the flow range experienced.

Additional data on 8-cm ion thruster and power processor hardware may be found in References 4, 6, and 13.

#### 2.4.2 Sensitivity Analysis

A sensitivity analysis was conducted to determine the sensitivity to total cost of the various individual cost elements. Tables 13 and 14 show the results from this analysis. Based on the MMS mission model shown in Reference 1, three modules were needed for the geosynchronous HPPM mission. There were no specific requirements for the low earth orbit HPPM. Accordingly, the sensitivity analysis was performed for  $n = 1, 2$ , and 3 for the synchronous HPPM mission, and for  $n = 1, 5$ , and 10 for the low earth orbit mission where  $n =$  the number of modules required. In Tables 13 and 14, the sensitivity to total cost for a 10% change in each cost element is shown. Wherever sensitivity exceeds 1%, it is underlined in the tables. Thus, the cost drivers are readily identified.

#### 2.5 BASELINE COMPARISON WITH SPS

In addition to the hardware and programmatic cost elements considered above, a comparison with the standard monopropellant hydrazine propulsion modules used on MMS must take into account Space Transportation System (STS) charges and propellant costs. The only differences in STS charges for the missions considered occur in Shuttle delivery to 160 nmi (300 km) parking orbit. In order to determine the applicable charges, the MMS characteristics per Reference 1 were employed. The dedicated Shuttle price was taken from Reference 14. When adjusted to 1978 dollars, it came to \$22.3 million. Shuttle charge factors were calculated from the charge algorithm shown in Reference 15, and were based on the larger load factor as determined from either payload weight or payload length in the cargo bay.

Table 13. Sensitivity of Total Cost to HPPM Cost Elements, Synchronous Mission

Item	n = 1		n = 2		n = 3	
	NR	R	NR	R	NR	R
Hardware						
Thruster and Gimbal Assembly	0.61	0.60	0.49	0.97	0.41	<u>1.21</u>
Propellant Storage and Distribution	0.14	0.11	0.11	0.18	0.10	0.22
Power Electronics Unit	<u>2.35</u>	0.66	<u>1.89</u>	<u>1.05</u>	<u>1.58</u>	<u>1.32</u>
Digital Controller and Interface Unit	<u>1.54</u>	0.41	<u>1.24</u>	0.66	<u>1.03</u>	0.82
Structure and Thermal Control	0.39	0.09	0.31	0.14	0.26	0.18
Integration and Assembly	0.39	0.27	0.31	0.44	0.26	0.55
Boost Regulator	0.24	0.13	0.19	0.21	0.16	0.26
DC-DC Converter	0.18	0.05	0.15	0.08	0.12	0.10
Additional Solar Array	0.13	0.07	0.10	0.11	0.08	0.14
Programmatic						
Aerospace Ground Equipment	0.92	<0.01	0.74	0.01	0.62	0.02
Launch Operations	0.03	<0.01	0.03	<0.01	0.02	<0.01
Development Tests	0.08	<0.01	0.07	<0.01	0.06	<0.01
Qualification Tests	0.09	<0.01	0.07	<0.01	0.06	<0.01
Subsystem Engineering	0.33	0.02	0.27	0.03	0.22	0.04
Reliability and Quality Assurance	0.10	0.16	0.08	0.25	0.07	0.31
Project Management	0.61	0.19	0.49	0.31	0.41	0.39

Sensitivity (%) of total cost to a 10% change in each cost element is listed for

n = number of modules required

NR = nonrecurring element

R = recurring element

Table 14. Sensitivity of Total Cost to HPPM Cost Elements, Low Earth Orbit Mission

Item	n = 1		n = 5		n = 10	
	NR	R	NR	R	NR	R
Hardware						
Thruster and Gimbal Assembly	0.57	0.57	0.27	<u>1.35</u>	0.16	<u>1.63</u>
Propellant Storage and Distribution	0.21	0.19	0.10	0.44	0.06	0.53
Power Electronics Unit	<u>2.21</u>	0.62	<u>1.05</u>	<u>1.47</u>	0.63	<u>1.77</u>
Digital Controller and Interface Unit	<u>1.45</u>	0.38	0.69	0.91	0.41	<u>1.10</u>
Structure and Thermal Control	0.37	0.08	0.17	0.20	0.10	0.24
Integration and Assembly	0.41	0.31	0.20	0.72	0.12	0.87
Boost Regulator	0.22	0.12	0.11	0.29	0.06	0.35
DC-DC Converter	0.17	0.05	0.08	0.11	0.05	0.13
Additional Solar Array	0.12	0.28	0.06	0.66	0.03	0.80
Additional Battery	0.03	0.13	0.01	0.30	0.01	0.36
Programmatic						
Aerospace Ground Equipment	0.87	<0.01	0.41	0.02	0.25	0.02
Launch Operations	0.03	<0.01	0.01	<0.01	<0.01	<0.01
Development Tests	0.08	<0.01	0.04	<0.01	0.02	<0.01
Qualification Tests	0.04	<0.01	0.02	<0.01	0.01	<0.01
Subsystem Engineering	0.31	0.02	0.15	0.05	0.09	0.06
Reliability and Quality Assurance	0.10	0.18	0.05	0.42	0.03	0.51
Project Management	0.58	0.22	0.27	0.53	0.17	0.63

Sensitivity (%) of total cost to a 10% change in each cost element is listed for

n = number of modules required

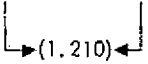
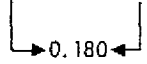
NR = nonrecurring element

R = recurring element

The recurring cost comparison between the HPPM and the SPS modules is shown in Table 15. Recurring cost estimates for the SPS modules were taken from Reference 11 (and adjusted to 1978 dollars). The synchronous HPPM module is compared with SPS-I, because the small impulse module can perform the baseline mission. It cannot, however, satisfy the low earth orbit mission requirements. Thus, the large impulse SPS-II module is compared with HPPM for the low earth orbit mission. Shuttle charges in all cases were based on load factor by length. As can be seen from Table 15, Shuttle charges are equal for SPS-I and HPPM, because they are both the same length. SPS-II, however, is 3.5 feet (1.1 m) longer, and has a correspondingly higher charge. The baseline cost comparison for the geosynchronous mission shows that HPPM recurring costs are \$1.210 million more than SPS-I. The baseline cost comparison for the low earth orbit mission shows that HPPM recurring costs are \$0.180 million less than SPS-II.

The sensitivity of HPPM and SPS recurring costs to Shuttle price is shown graphically in Figure 10. If, for example, the dedicated Shuttle price were to go up to \$24.5 million (about 10% more than the baseline

Table 15. Baseline HPPM Recurring Cost Comparison with SPS (\$ Millions)

	SPS-I	HPPM SYNCHR	SPS-II	HPPM LOW EARTH
RECURRING COST	0.882	2.093	0.961	2.523
HYDRAZINE PROPELLANT	<u>0.001</u>		<u>0.003</u>	
SUB TOTAL	0.883	2.093	0.964	2.523
SHUTTLE CHARGES FOR 160 N. M1 (a)	<u>5.709</u>	<u>5.709</u>	<u>7.448</u>	<u>5.709</u>
TOTAL	6.592	7.802	8.412	8.232
Δ COST				

(a) ASSUMES 6 FT. LONG PAYLOAD

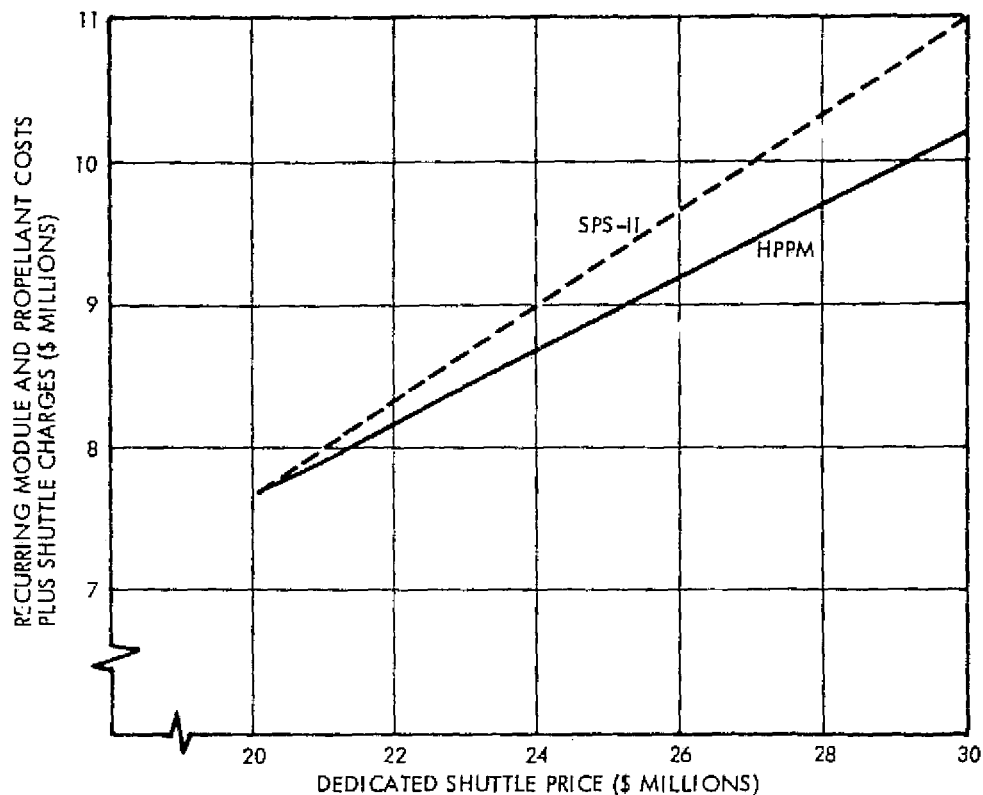


Figure 10. HPPM and SPS Sensitivity to Shuttle Price

value used), then HPPM recurring costs would be about \$0.350 million less than SPS-II.

## 2.6 COST REDUCTION STUDIES

From the discussion in the preceding sections, it is clear that the HPPM cost drivers are:

- Shuttle charges
- Power processing (PEU, DCIU, boost regulator, dc-dc converter)
- Thruster and gimbal assembly

In order to investigate means for reducing the impact of these cost drivers, a series of cost reduction tradeoffs was conducted. Table 16 lists the studies performed. Each one is discussed separately below.



Table 16. HPPM Cost Reduction Studies

Designation	Description
8-1	Unregulated 28 Vdc Input to Power Processor
8-2	Time Sharing DCIU
8-3	PEU Output Switching
8-4	Combination of 8-1, 8-2, and 8-3
8-5	Extended Stationkeeping Mission

#### 2.6.1 Unregulated 28 Vdc Input to Power Processor

The baseline HPPM power processor requires both unregulated 70-volt and regulated 28-volt input power (see Sections 2.3.4 and 2.3.5). The power processor can be redesigned to operate directly from the unregulated 28 Vdc MMS bus. Thus, the boost regulators and dc-dc converters from the baseline power subsystem would be eliminated.

The redesigned PEU will have an electrical efficiency reduction of 3% for handling the unregulated 28 Vdc input. This, however, is an improvement over the losses existing in the baseline combination of power processor and boost regulator. The approximate PEU power increase is 7 watts, and weight increase is 0.5 kg (1.1 lb). The increased nonrecurring cost of the power processor is estimated at \$167 thousand. The recurring HPPM cost reduction is \$148 thousand.

#### 2.6.2 Time Sharing DCIU

The DCIU can be redesigned so that it may be time shared between the four power electronic units. A standby redundant DCIU would be available to operate the thrust subsystem in case of primary unit failure. Thus, two DCIUs are eliminated (four are used in the baseline HPPM).

The redesigned DCIU should weigh 0.4 kg (0.9 lb) more than the baseline unit, and require an additional 2 watts of power. The nonrecurring design cost for DCIU modification is about \$250 thousand more than baseline costs.

The recurring HPPM cost reduction is \$176 thousand.

### 2.6.3 PEU Output Switching

Instead of dedicating a power processor to each thruster, a relay network as shown in Figure 11 illustrates how three power processors may be used to operate four thrusters. Each primary thruster still has its own redundant unit, but each primary power processor now shares a single redundant unit. Nine high voltage relays at each switching location are required to switch 8-cm thruster PEU outputs (11 relays are required for the 30-cm power processor). Two sets of relays are used to switch between primary and redundant ion engines. An additional two sets of relays are used to switch between the primary power processors and the single redundant unit. In all, 36 relays are contained in the HPPM switch box.

As recommended in Reference 4, the Kilovac HC-1/S41 relay is used for this application. It is rated at 2.5 kV, and its contacts have a current carrying rating of 18 amperes. The interrupt current rating is 3 amperes, and therefore, cannot be switched when the power processor is on. The power processor must be commanded off before any commands

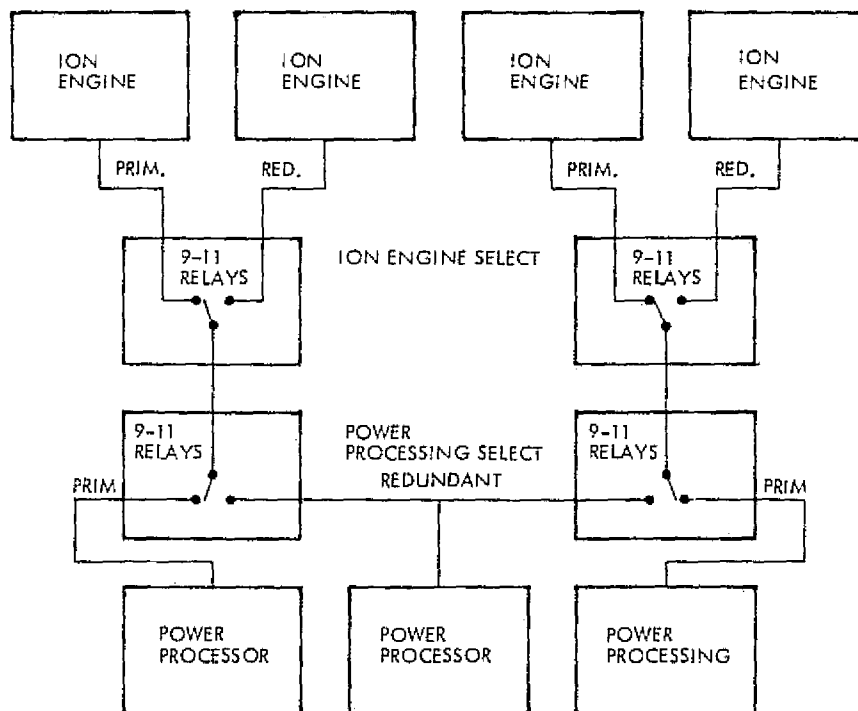


Figure 11. Output Switching Matrix

be sent to the relay matrix. The relays are nonlatching and require power to remain closed in the redundant position. The estimated power drain for holding each set of relays is 22.5 watts. In order to operate both redundant thrusters and the redundant power processor simultaneously requires an additional 67.5 watts to the HPPM.

By adding the output switch box to the HPPM, one PEU, one DCIU, and one boost regulator are eliminated. The switch box weighs 3.0 kg (6.6 lb). The nonrecurring cost for the switch box is \$88 thousand. The unit recurring switch box cost is \$22 thousand.

The resulting recurring HPPM cost reduction for incorporating an output switch box is \$208 thousand.

#### 2.6.4 Unregulated 28 Vdc Input, Time Sharing DCIU, and PEU Output Switching

The recurring cost breakdown in Table 17 is presented for incorporating unregulated 28 Vdc input to the power processor, time shared DCIUs, and PEU output switching in the HPPM for the low earth orbit mission. The combination of these cost reductions amounts to an HPPM recurring cost of \$2.103 million for a \$0.420 million total reduction.

Referring to Table 15, it is seen that the baseline HPPM recurring costs are \$0.180 million less than SPS for the low earth orbit mission. By incorporating the cost reductions identified above, HPPM recurring costs are \$0.600 million less than SPS, including propellant and Shuttle charges.

#### 2.6.5 Increased Mission Life, Synchronous HPPM

The baseline geosynchronous mission life is 3 years (see Table 1). The effects of increasing mission duration, to provide up to 7 years stationkeeping and other auxiliary propulsion functions, are shown in Table 18. The most significant thing to note is that the SPS configuration changes from SPS-I to SPS-II between 3 and 4 years mission life requirement because the hydrazine propellant load exceeds SPS-I capacity. The largest effect of this configuration change is to increase SPS Shuttle charges from \$6.592 to \$8.410 million.

Table 17. HPPM (Designation 8-4) Recurring Cost Breakdown, Low Earth Orbit Mission

- Unregulated 28 VDC input
- Time sharing DCIU
- PEU output switching

Item	Unit Cost (\$ millions)	Quantity	Total (\$ millions)
Hardware			
Thruster and Gimbal Assembly	0.112	4 ea	0.448
Propellant Storage and Distribution	---	1 set	0.147
Power Electronics Unit	0.123	3 ea	0.369
Digital Controller and Interface Unit	0.076	2 ea	0.152
Structure and Thermal Control	---	As req'd	0.067
Integration and Assembly	---	As req'd	0.241
Additional Solar Array	---	11 m <sup>2</sup>	0.240
Additional Battery	0.100	1 ea	0.100
Output Switch Box	0.022	1 ea	0.022
Programmatic			
Aerospace Ground Equipment			0.007
Subsystem Engineering			0.017
Reliability and Quality Assurance			0.125
Project Management			0.168
Total			2.103

Table 18. Increased Mission Life, Synchronous HPPM

Mission Duration, yr	3	4	5	6	7
Hydrazine Weight, lb	185	248	308	370	433
SPS Configuration	I	II	II	II	II
SPS Recurring Cost, \$M	0.882	0.961	0.961	0.961	0.961
N <sub>2</sub> H <sub>4</sub> Cost, \$M	0.001	0.001	0.002	0.002	0.002
Shuttle Charges, \$M	<u>5.709</u>	<u>7.448</u>	<u>7.448</u>	<u>7.448</u>	<u>7.448</u>
Total, \$M	6.592	8.410	8.411	8.411	8.411
HPPM Baseline Recurring Cost, \$M	2.093	2.132 <sup>(a)</sup>			
Hg Cost, \$M	<0.001	← <0.001 →			
Shuttle Charges, \$M	<u>5.709</u>	<u>5.709</u>			
Total, \$M	7.802	7.841			
Δ Cost, SPS-HPPM, \$M	(1.210)	0.569	0.570	0.570	0.570
Δ Wt. Cost to Synchronous Orbit, <sup>(b)</sup> \$M	0.314	0.650	0.760	0.874	0.990
Cost Reduction, Designation 8-4 (per Section 2.6.4)	← 0.420 →				
Total Δ, \$M	(0.476)	1.639	1.750	1.864	1.980

(a) Assumes dedicated solar array for 7 yr

(b) IUS ≈ \$10M/5000 lb = \$2K/lb

In order to simplify HPPM recurring cost analysis, it was assumed that a dedicated solar array would be available to the HPPM for up to 7 years. Other HPPM costs nominally remained the same, because increased mercury propellant requirements did not alter the module configuration.

From Table 18, it may be seen that the recurring cost difference between SPS and HPPM changes from a more expensive to a cheaper recurring cost for HPPM when mission life is 4 years or more. In addition, if the weight margin provided by HPPM could be converted to useful geosynchronous payload, it is worth about \$2000 per pound (\$4400 per kg) for each additional pound of payload based on the assumption that the Interim Upper Stage (IUS) costs \$10 million to deliver 5000 pounds (2270 kg) to synchronous orbit. Further, the cost reductions discussed in Section 2.6.4 are also applicable to the geosynchronous HPPM configuration, yielding an additional \$0.420 million reduction. The sum of all these considerations is shown at the Total  $\Delta$  (bottom) line on Table 18. For a 4-year geosynchronous mission, the recurring HPPM cost is \$1.639 million less than SPS-II, including propellant and Shuttle charges, payload margin savings, and incorporation of cost reductions identified for HPPM Designation 8-4.

### 3. ION PROPULSION MODULE FOR SUN-SYNCHRONOUS SATELLITE SERVICING

From an overall mission operation standpoint, on-orbit servicing of spacecraft has great potential for saving money. On-orbit servicing is among the factors which influenced the inception and design of the MMS. Current interest in servicing is limited primarily to low-altitude missions. On-orbit servicing typically involves replacing one or more modules on the spacecraft, which could include replacing the propulsion module.

#### 3.1 SUN-SYNCHRONOUS MISSION

The key characteristic of a sun-synchronous satellite is that the earth under the satellite is always viewed with the same lighting conditions. In other words, the angle between the plane of the orbit and the sun's rays is constant. The altitudes of sun-synchronous orbits generally range from 500 to 900 km (roughly 270 to 490 nmi). It can be shown, in this altitude range (Reference 1), that these orbits have inclinations around 98 to 99 degrees.

The Shuttle parking orbit is close to 300 km (160 nmi). Most of the propulsive requirements for servicing sun-synchronous satellites are those for going between the Shuttle orbit and the desired spacecraft orbit. Three distinct trajectory segments have been identified for sun-synchronous servicing. These are: (1) to deploy the spacecraft, (2) to return it to Shuttle for servicing, and (3) to replace the serviced spacecraft at operational altitude. In addition to these requirements, there are on-orbit velocity requirements, e. g., for attitude control.

The strategy adopted in Reference 1 for servicing sun-synchronous satellites assumed that they would be serviced by Shuttle flights in approximately 100-degree inclined orbits. This means that sun-synchronous satellites would be serviced by flights which launch other sun-synchronous satellites. In general, bringing a sun-synchronous satellite down to a 300-km shuttle parking orbit for servicing will require that the satellite's orbit altitude, inclination, and longitude of ascending node all be changed to match that of the Shuttle orbit. This may be accomplished by placing the satellite in an intermediate parking orbit whose node will precess to

the proper location by the time the Shuttle arrives on orbit. There will be an optimum altitude for the parking orbit to minimize the total  $\Delta v$  required to bring the satellite down.

After servicing is completed, the satellite must be replaced in its original orbit. The technique for this is similar to that for bringing it down. The satellite is placed in a parking orbit which precesses it to the desired line of nodes. It is then transferred to the final orbit.

When comparing this strategy for low-thrust servicing with chemical systems, the following findings were reported:

- 1) The mission times on the return to Shuttle trajectories for low thrust are comparable to those of the chemical systems, and for both systems are less than 4 months (the minimum time assumed for fitting into Shuttle scheduling).
- 2) The mission times to return to the desired orbit after being serviced by Shuttle when a shift in longitude of nodes has occurred are approximately the same (or slightly longer) for ion systems as for chemical systems (3 to 6 months).
- 3) The mission time on the initial delivery leg is significantly longer for ion systems than for chemical systems (22 days for ion systems versus a few hours for chemical systems for a 900-km final orbit).
- 4) Ion propulsion systems have less flexibility with regard to reacting to Shuttle launch delays than chemical systems.
- 5) The propellant mass requirements for ion propulsion systems are significantly less than for chemical systems (15 to 60 kg per trajectory segment for ion systems versus 160 to 500 kg per trajectory segment for chemical systems).

Based upon these comparisons, the major advantage of ion propulsion is the smaller propellant masses required. The traditional disadvantage of ion propulsion, long mission times, did not appear to be a disadvantage for the sun-synchronous application, with the possible exception of the initial deployment. Another potential application in the sun-synchronous mission area which uses the best advantages of the ion propulsion, low propellant mass requirements, is the change of on-orbit viewing conditions in addition to placement, retrieval and servicing of the satellite.



### 3.2 CONFIGURATION

The propulsion subsystem schematic for sun-synchronous satellite servicing is shown in Figure 12. The subsystem incorporates four 30-cm ion thrusters and their associated equipment. Each thruster is gimbal mounted, and accepts conditioned power from a power processing unit. The 30-cm thruster has been designed with a 4:1 throttling capability. At full thrust, it is rated at 29 millipounds (129 millinewtons) and 2900 seconds specific impulse (Reference 16). Thruster design details are given in Reference 17. The gimbal mechanism is described in Reference 18, and the power processor is described below. The propellant storage and distribution system is a derivative of the approach employed for the SERT II spacecraft, as described in Reference 18. The tank is sized to hold 180 kg of mercury plus 15% contingency reserve, in order to meet the sun-synchronous mission requirements discussed in Section 3.1 over a pressure blowdown range of 3:1.

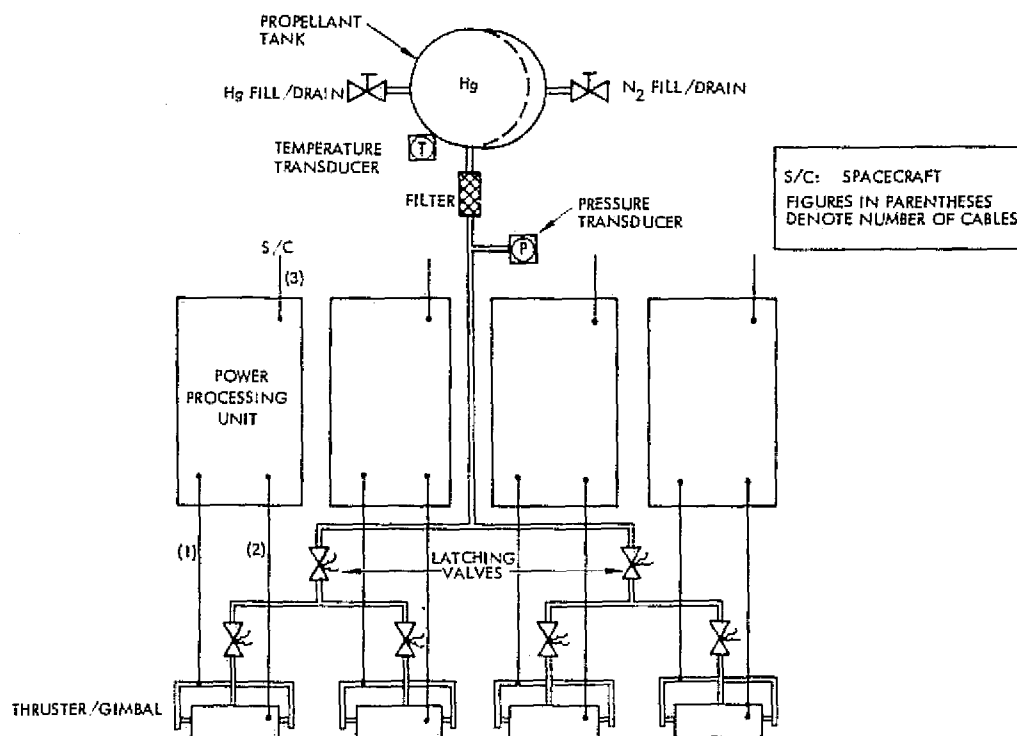


Figure 12. Propulsion Subsystem Schematic for Sun-Synchronous Satellite Servicing

### 3.2.1 30-cm Ion Thruster Power Processor

The 30-cm ion engine power processor is presently in the prototype phase (References 19 and 20). The electrical prototype power processor is packaged into seven modules as shown in Figure 13. Each module can be assembled and tested individually. The modular construction permits electrical design changes to be easily incorporated in a particular module without any impact on the other modules. NASA-Lewis Research Center has been performing detail mechanical packaging of the functional model power processor, as reported in Reference 20.

Figure 14 shows the 30-cm power processor block diagram. It identifies all of the internal electrical functions with the mechanical sub-assembly designations.

The main input power is from the 200 to 400 Vdc solar array bus. The dc power is filtered by the dc input filter to ensure meeting 170 rms

ORIGINAL PAGE IS  
OF POOR QUALITY

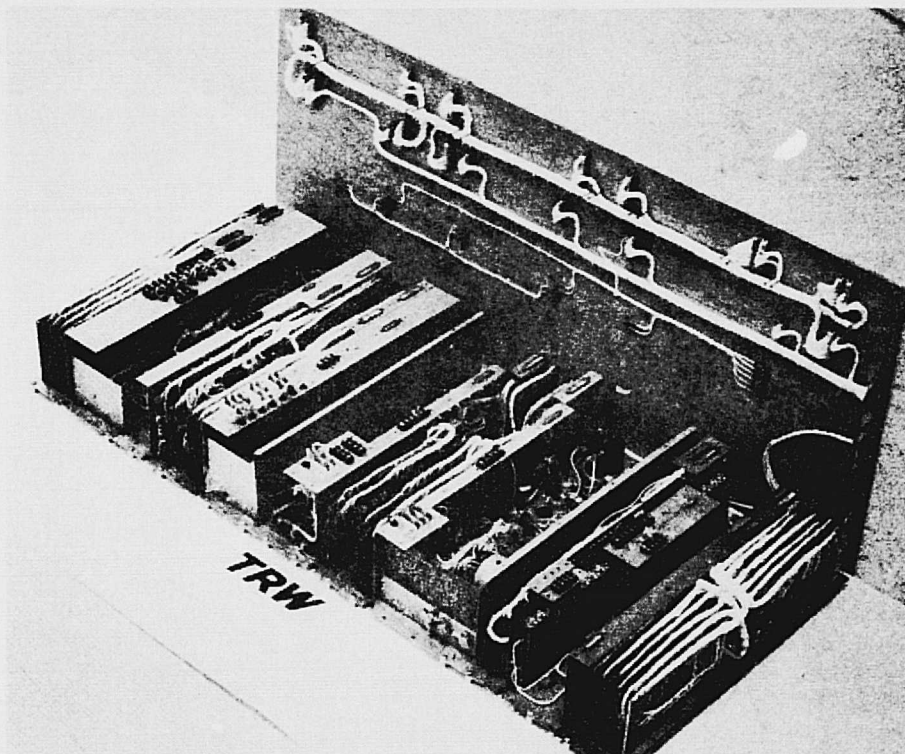


Figure 13. Electrical Prototype Power Processor for 30-cm Ion Engine Showing Modular Construction

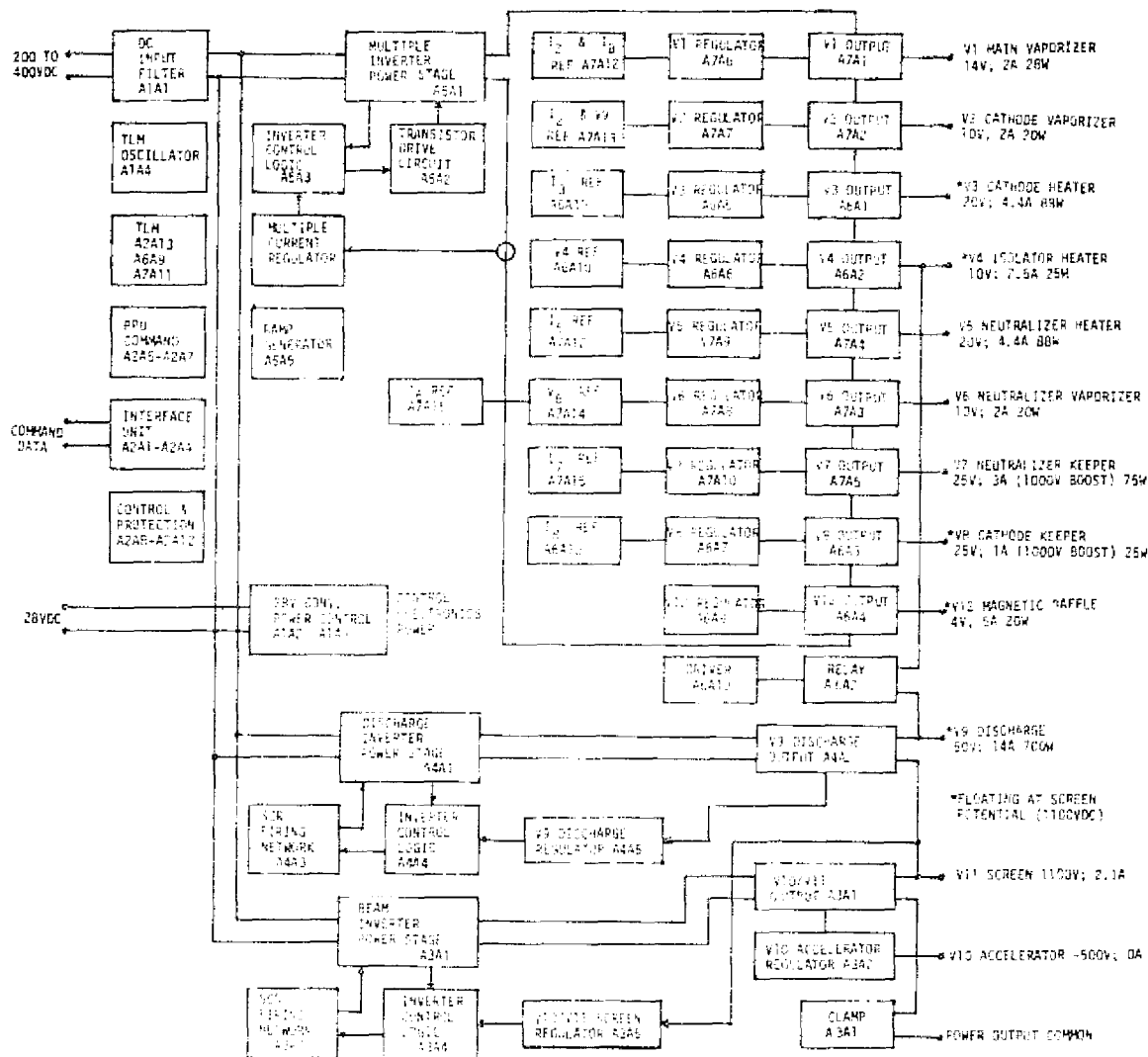


Figure 14. Power Processor Block Diagram

reflected input ripple from the power processor. The dc power flows to three series resonant inverters:

- Multiple inverter power stage (50 kHz transistor)
- Discharge inverter power stage (20 kHz thyristor)
- Beam inverter power stage (20 kHz thyristor)

ORIGINAL PAGE IS  
OF POOR QUALITY

The multiple inverter operates at 50 kHz in order to reduce the component weight of magnetics and output filter capacitor. The multiple inverter supplies power to the low voltage outputs:

- V1 main vaporizer
- V2 cathode vaporizer
- V3 cathode heater
- V4 isolator heater
- V5 neutralizer heater
- V6 neutralizer vaporizer
- V7 neutralizer keeper
- V8 cathode keeper
- V12 magnetic baffle

Each output has its own regulator electronics and commandable operating set points. The discharge inverter supplies power to the discharge output. The beam inverter supplies power to both the screen and accelerator outputs. With both of these outputs on a common output transformer, power can be shared in any manner during start-ups to clear the screen/accelerator electrodes of the ion engine and to form the ion beam.

The power processor is controlled by the digital interface unit which establishes the power processor unit commands. It receives serial input data and provides parallel output command lines.

Internal control and protection electronics sense arcs on the ion engine and perform the recycling to again establish an ion beam. The input power bus voltages are also monitored to ensure turnoff in case of abnormal input line conditions.

Telemetry monitoring is provided for the power processor unit to establish thruster system operating parameters. Unregulated 28 Vdc power goes through the 28 Vdc-dc converter and powers all of the internal control electronics.

The power processor employs five separate grounds. These are:

- 200 to 400 Vdc power bus
- 28 Vdc power bus
- Ion engine structure

- Digital interface unit
- Spacecraft computer

The power processor is designed to operate with a center tapped power source or the negative power terminal grounded. Ground isolation is provided by transformer winding isolation in the power stages. The power processor regulator electronics and telemetry conditioning isolation is provided by magnetic sensors and optical couplers. The spacecraft computer drives optical couplers in the digital interface unit. The return data to the spacecraft computer is isolated by optical couplers in the spacecraft computer.

Preliminary design work (Reference 10) has been performed to incorporate a microprocessor into the digital interface unit and limits the use of the spacecraft computer for thrust system operation.

The present power processor design has 27 telemetry monitors, 69 discrete on/off and set point commands, and four 128 step command references for beam current, discharge current, magnetic baffle current, and screen supply output voltage.

The baseline 30-cm ion thruster power processor for the sun-synchronous satellite servicing mission is a modification of the present electrical prototype power processor described in Reference 21. Figure 15 shows the power processor block diagram. It is similar to the previous unit, except for the following changes:

- Use of the V9 discharge supply for V3 cathode heater and V4 isolator heater during ion engine start-up
- Elimination of digital interfaces because of reduced command and telemetry requirements

The power processor includes a common first stage dc input filter and a separate second stage dc input filter for the three power inverters used to process the unregulated 200 to 280 Vdc solar array bus in order to meet the ion engine power, control, and regulation requirements. The inverters include the beam inverter for the screen/accelerator output; discharge inverter for the discharge output; and the multiple inverter. The multiple inverter supplies 50 kHz ac power to the low power ion engine loads. A separate dc-dc converter processes the unregulated 28 Vdc bus

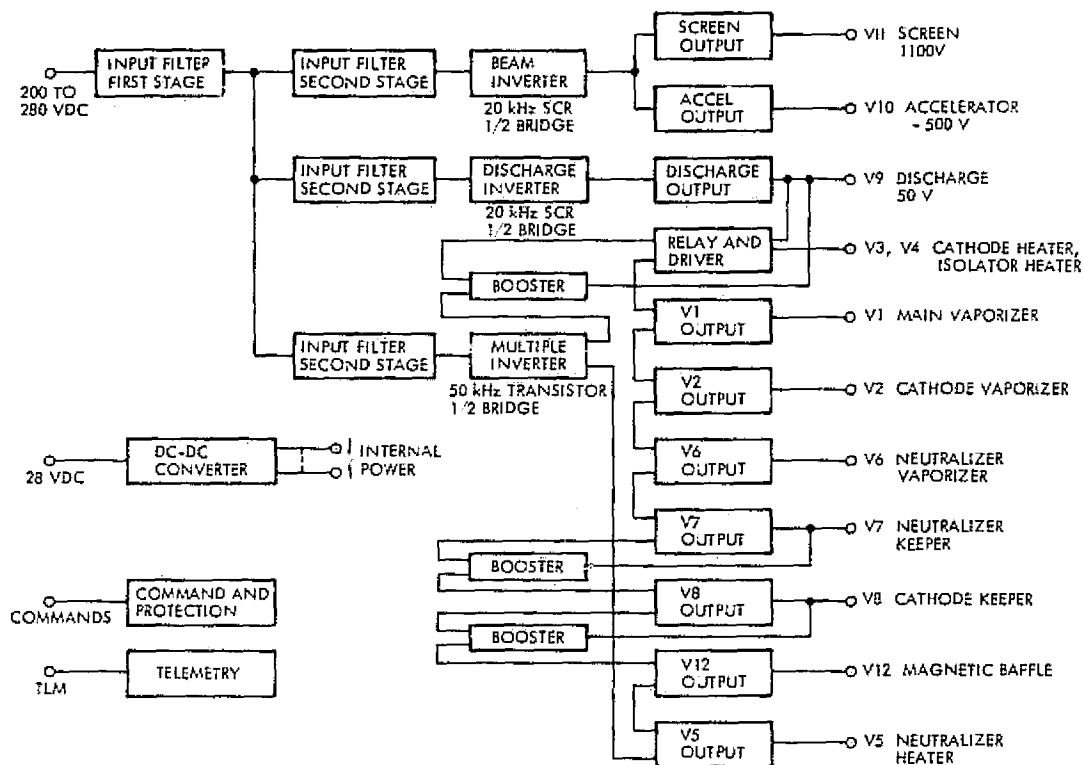


Figure 15. Baseline 30-cm Thruster Power Processor Block Diagram

and supplies power to the power processor internal control electronics. The command and protection functions control the start-up of the power processor and provide protection during ion engine overload and during abnormal input bus voltage. The telemetry monitors evaluate the performance of the ion thruster. The commands use optical isolation and the telemetry has magnetic isolation to eliminate ground loop current during abnormal or transient ion thruster operating modes. Table 2 (Section 2.3.1) lists the necessary command and telemetry requirements for the thrust subsystem, excluding thruster gimbal control.

Based upon the results of Reference 10, a revised estimate of the baseline power processor characteristics is presented in Table 19, and is compared with the functional model in Table 20. The design changes for the baseline include the following:

- Elimination of power supplies for V3 cathode heater and V4 isolation heater
- Elimination of digital interface electronics

Table 19. Estimate of Baseline 30-cm Thruster Power Processor Characteristics

	Part Count	Weight (gms)	Losses (W)	Efficiency (%)
Beam Inverter (2200 W)				
Power stage	59	4,803	162.0	93.1
SCR firing	74	87	13.1	
Series inverter control	125	116	1.4	
Regulator	92	121	2.1	
Accelerator regulator	71	108	4.0	
Beam Total	421	5,235	182.6	
Discharge Inverter (415 W)				
Power stage	33	2,966	56.5	88.0
SCR firing	74	87	13.1	
Series inverter control	125	116	1.4	
Regulator	97	132	1.1	
Discharge Total	329	3,301	72.1	
Multiple Inverter (45 W) (Series Inverter)				
Power stage	10	207	15.5	46.0
Controls	319	362	10.2	
Outputs —				
Power	146	1,523	37.1	
Regulators	526	593	3.0	
Multiple Total	1001	2,685	65.8	
Input Filter	32	2,147	8.2	
Subtotals	1783	13,368	328.7	89.0
Telemetry	120	300	3.5	
Protection	235	186	3.0	
Command	52	182	2.6	
28 Volt converter	122	612	16.4	
Output Power = 2660 W Totals	2312	14,648	354.2	88.2

Table 20. Power Processing Unit Characteristics for 30-cm Ion Thruster

	Functional Model	Baseline
Weight, kg (lb)	36.2 (79.7)	29.2 (64.3)
Input Power at 240 $\pm$ 40 Vdc, watts	2996	2944
Input Power at 28 $\pm$ 7 Vdc, watts	100	70
Power Conversion Efficiency, %	87	88
Size, inches (cm)	6 x 18 x 45 (15.2 x 45.7 x 114.3)	6 x 18 x 40 (15.2 x 45.7 x 101.6)
Part Count	3998	2312

- Use of integrated circuits for regulator control electronics
- Elimination of circuit redundancy

Each major power processor function is identified and part count, weight, and power losses are estimated in Table 19. The total baseline power processor part count is 2312. The electrical component weight is 14.6 kg and the projection of the packaged weight is 29.2 kg. The estimated size is 18 inches wide by 40 inches long by 6 inches high (45.7 x 101.6 x 15.2 cm). The total overall power processor efficiency is 88.2% with 70 watts input from the 28 Vdc bus and 2944 watts from the 200 to 280 Vdc bus.

### 3.2.2 Thruster Performance Requirements

For the sun-synchronous mission, the 30-cm thrusters are fired in pairs during placement, retrieval, and servicing trajectory segments. Two thrusters are kept in standby redundancy. According to Reference 1, the trajectory segment from a 300 km Shuttle parking orbit to a 900 km operational orbit requires approximately 37 days, including shadowing during the thrust phase for a 950 kg spacecraft. Depending on the local crossing time of the ascending node, the spacecraft could be shadowed on



each orbit. The average orbital period from 300 to 900 km is 1.6 hours, which requires the thruster pairs to cycle about 15 times a day for shadowed transfer orbits. Assuming that the on-orbit attitude control subsystem momentum wheels are sized to permit daily unloading, one thruster will be required to unload the wheels for about 15 minutes each day. The longest sun-synchronous mission listed in Reference 1 lasts 5 years. Thus, the maximum number of thruster cycles is (three trajectory segments) (15 cycles/day) (37 days) plus (365 cycles/year) (5 years) which equals 3490 cycles, which is 490 cycles above the 3000 cycle design life for a 30-cm thruster (Reference 16). In this case, two thrusters would have to share momentum wheel unloading to stay within design limits. One alternative would be to size the momentum wheels for unloading at less frequent intervals.

The propellant throughput to operate for the design life of a 30-cm thruster is 240 kg (Reference 16). Since the propulsion module contains only 180 kg (excluding reserve), the thrusters will be operating well within lifetime limits.

### 3.2.3 Propulsion Module Layout and Interfaces

The layout drawing for the sun-synchronous satellite servicing propulsion module is shown in Figure 16. An isometric view of the module is presented in Figure 17. Thermal insulation, fluid valves and fittings, electrical cabling and harness were omitted from the isometric view for clarity. The module contains four 30-cm thrusters, which are fired in pairs for orbit transfer maneuvers. Each thruster has its own gimbal assembly, and receives mercury propellant from a central storage and distribution tank. Each thruster has its own power processing unit.

The thermal control to dissipate approximately 350 watts from each operating power processor consists of six variable-conductance heat pipes transmitting the heat to a radiating surface which views cold space. As shown, two radiators and 24 heat pipes are used. Thermal insulation blankets the power processors, propellant tank, and gimbals. The thrusters and radiators protrude through the blanket. With the thrusters off, the variable-conductance heat pipes effectively block heat transfer from power processing units inside the blanketed region out to cold space.

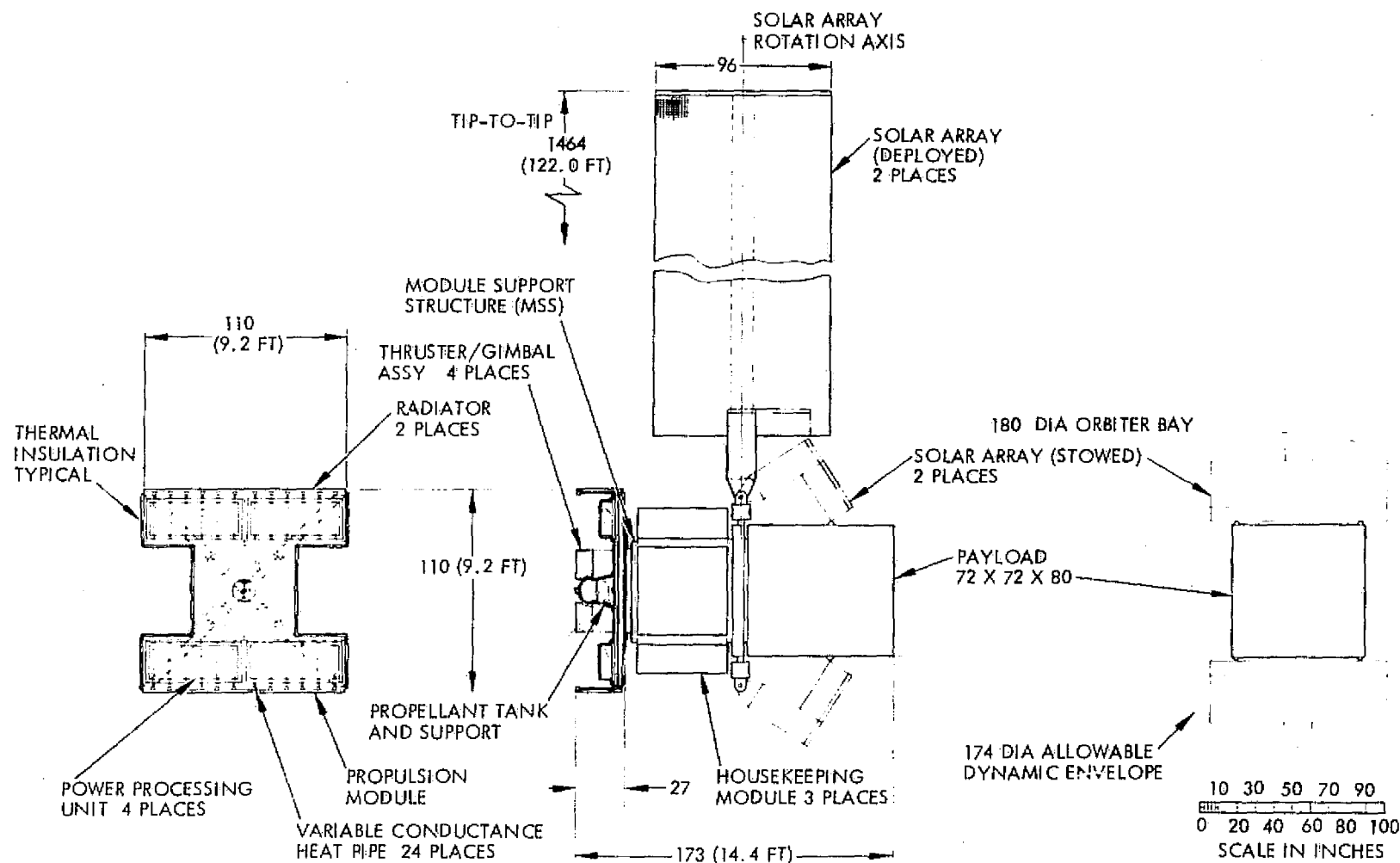


Figure 16. Layout of Sun-Synchronous Satellite Servicing Propulsion Module for MMS

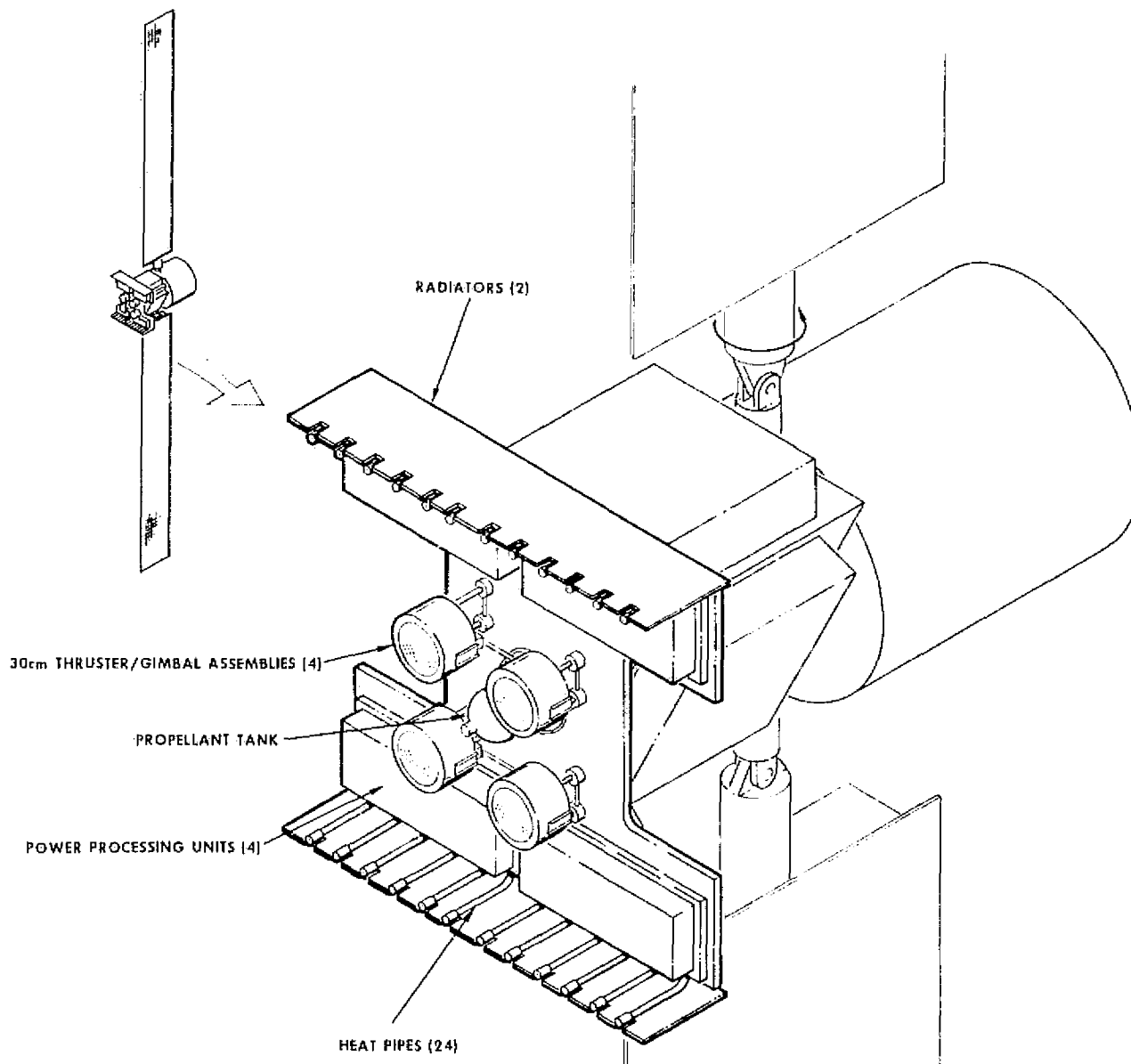


Figure 17. Propulsion Module for Sun-Synchronous Satellite Servicing

Thermal control is required for the 30-cm subsystem because of its large heat dissipation requirements. The HPPM using 8-cm thrusters has modest heat dissipation requirements, and, consequently, does not require heat pipes and radiators for thermal control.

The large input power requirements for the thrusters necessitate large solar arrays. Array sizing is discussed below in Section 3.2.6. The layout drawing, Figure 16, illustrates a typical stowage and deployed array configuration. Two symmetrical array panels are employed, spanning 122 feet tip-to-tip when deployed. Array rotation about one-axis is provided for sun-pointing during orbit transfer. It is assumed that there will be only minor interactive effects between the nominally 240-volt array and its surroundings.

During the periods of orbit transfer, the orbit does not remain sun-synchronous. Thus, the most general condition regarding sun line orientation relative to the spacecraft body axes during the thrust phase must be addressed. It can be shown, however, that a single-axis articulation of the solar array plus a spacecraft body rotation about the principal thrust vector axis is sufficient to produce maximum solar array output during thrust phases. Note that the payload is not necessarily earth-pointing during orbit transfer, permitting spacecraft body rotation during these time periods.

The single-axis solar array articulation concept adopted has the further advantage that spacecraft surfaces normal to the array rotation axis will not be sun-illuminated during the thrust phase and thus provide a favorable location for the power processing unit radiators. The layout therefore uses radiator panels of only about half the area that would otherwise be required, i. e., if exposed to the sun part of the time.

Several factors have been considered to assure that the propulsion module is compatible with the Shuttle. These factors were also considered for the HPPM and are identified in Section 2.3.2. The only difference is that the propellant tank represents a single point failure, but, because this approach was adopted for the SPS-II propulsion module, it was also retained for the present case.

The support ring on the propulsion side of the MMS module support structure (MSS) provides the mechanical interface to cruciform support beams on the propulsion module. Except for Shuttle launch loads, no significant loads need to be accommodated by this interface. The solar array is structurally attached to the payload adapter ring at the other end of the MSS to reduce potential exposure to thruster exhaust products.

#### 3.2.4 Propulsion Subsystem Weight

The ion propulsion subsystem dry weight breakdown for sun-synchronous satellite servicing is shown in Table 21.

#### 3.2.5 Propulsion Subsystem Electrical Interface

The electrical interfaces between the propulsion subsystem and the MMS are presented in Table 22. The power subsystem interface is discussed in more detail in the next subsection. The command and data handling interface is straightforward and requires no further comment.

Table 21. Ion Propulsion Subsystem Weight, Sun-Synchronous Satellite Servicing Mission

Hardware	Unit Mass (kg)	No. Required	Mass (kg)	Weight (lbf)
Thruster and gimbal assembly	11.7	4	46.8	103.1
Propellant tank (a)	5.0	1	5.0	11.0
Power processing unit	29.2	4	116.8	257.3
Fill/drain valves	0.1	2	0.3	0.6
Latching valves	0.4	6	2.4	5.4
Filter	0.1	1	0.1	0.2
Pressure transducer	0.1	1	0.1	-
Propellant lines	-	1	(b)	-
Cables	-	28	8.9	19.6
Total Dry Weight			180.4	397.2

(a) Includes pressurant, temperature transducer

(b) Less than 0.1 kg

Table 22. Ion Propulsion Subsystem Electrical Interface,  
Sun-Synchronous Satellite Servicing

POWER	5900 WATTS AT $240 \pm 40$ VDC 140 WATTS AT $28 \pm 7$ VDC 8 WATTS AT 28 VDC FOR EACH GIMBAL MOTOR ACTUATION		
COMMANDS	FUNCTION	TYPE	NO. REQ'D.
	THRUSTER IDLE	DISCRETE	4
	THRUST ON	DISCRETE	4
	THRUST OFF	DISCRETE	4
	GIMBAL $\alpha +$	DISCRETE	4
	GIMBAL $\alpha -$	DISCRETE	4
	GIMBAL $\beta +$	DISCRETE	4
	GIMBAL $\beta -$	DISCRETE	4
	PROPELLANT VALVE	DISCRETE	4
	THRUSTER VALVE	DISCRETE	8
	TOTAL		40
TELEMETRY	SIGNAL	TYPE	NO. REQ'D.
	BEAM CURRENT	ANALOG	4
	BEAM VOLTAGE	ANALOG	4
	NEUTRALIZER EMISSION		
	CURRENT	ANALOG	4
	ACCELERATOR CURRENT	ANALOG	4
	TANK PRESSURE	ANALOG	1
	PROPELLANT TANK		
	TEMPERATURE	ANALOG	1
	LATCHING VALVE STATUS	BI-LEVEL	6
	TOTAL		24

### 3.2.6 Power Subsystem Configuration

In addition to its other functions, the power subsystem generates and distributes power to four ion engine power processors within the propulsion module. Power from the MMS power module is routed to the processor low voltage control circuits and remote power control switchgear used for fault isolation and power distribution. Power subsystem requirements are summarized in Table 23. The power processors operate only in sunlight to minimize energy storage requirements. The total power required by the processors is 5900 watts from the 240 Vdc solar array bus and 140 watts from the  $28 \pm 7$  Vdc bus in sunlight only. Design margin has been provided by sizing the subsystem for 6000 watts from the 240 Vdc bus and by permitting continuous low voltage control circuit operation in both sunlight and eclipse.

Table 23. Power Subsystem Design for the Propulsion Module - Requirements Summary

<u>Power Processors (each)</u>	
Input power	3000 watts
Input voltage	240 Vdc
Operation	In sunlight only
Fault isolation	External to processors
<u>Power Processor Low Voltage Control Circuits (each)</u>	
Input power	70 watts
Input voltage	28 $\pm$ 7 Vdc
Operation	Continuous
<u>Power Distribution</u>	
(a) Protect against faults at power processor input	
(b) Connect array to 2 of 4 power processors	
(c) Interface with high voltage array and low voltage MMS power bus.	

A simplified block diagram of the power processor interface is shown in Figure 18. The solar array consists of two wings, each of which is divided into high and low voltage sections. The high voltage sections feed the power processors through power distribution assemblies which contain solid state remote power controllers (RPCs) similar to those described in Reference 22. The RPCs require control power from the 28  $\pm$ 7 Vdc bus. The low voltage array sections provide power to the MMS power module to supply control circuit power and battery recharge energy. The low voltage section power output is sized only for propulsion module needs to clearly identify array weight and area associated with the propulsion module. In practice, the array would also include additional area to power payload and spacecraft subsystem equipment.

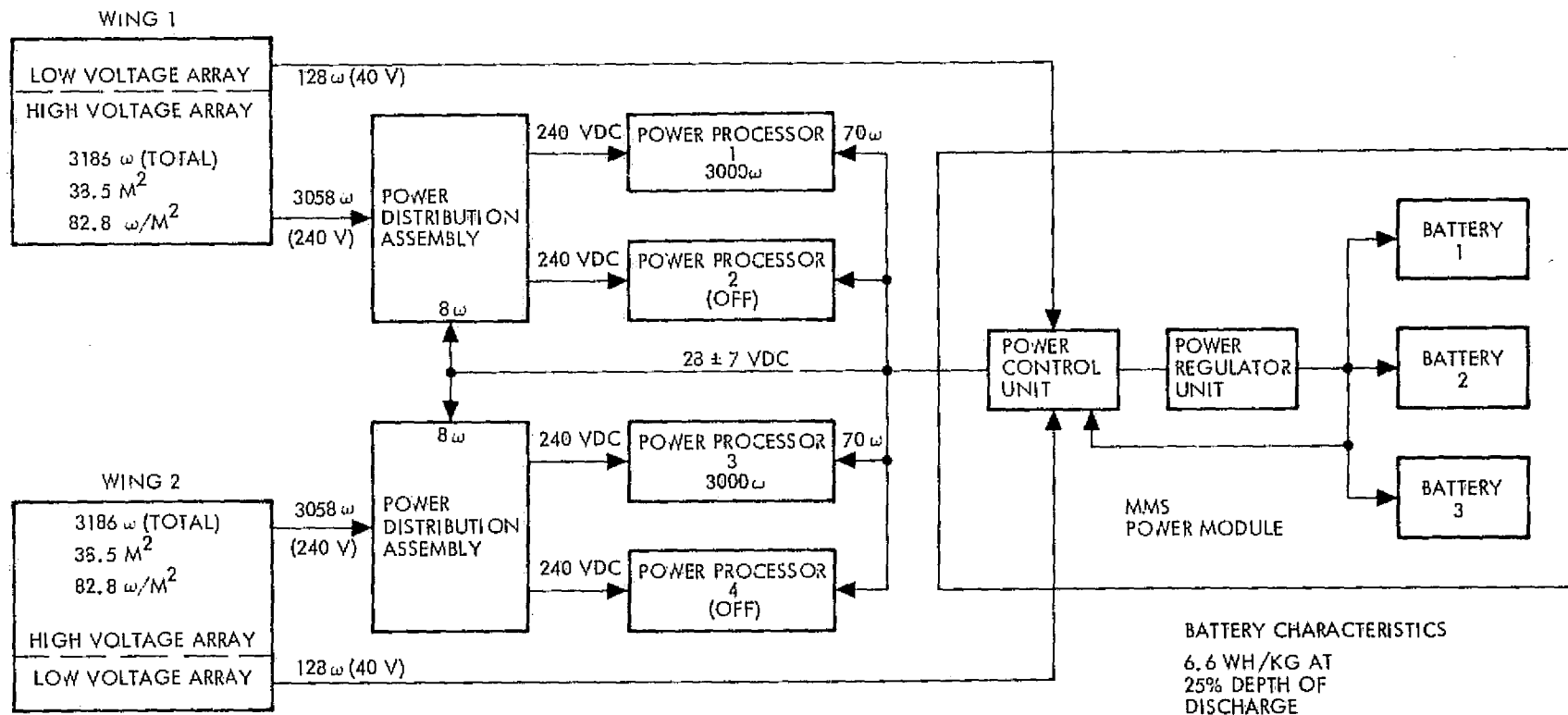


Figure 18. Power Processor to Solar Array Interface



### Solar Array Sizing

The solar array has been sized to provide the required power at five years in a 900 km altitude orbit inclined 100 degrees to the equator. The solar-electric propulsion (SEP) solar array characteristics as described in Reference 23 have been scaled to this application. Array power calculations assume use of high efficiency hybrid back surface reflector cells (11.4% efficiency at 28°C). The total trapped particle radiation fluence was calculated from Reference 24 as  $8.92 \times 10^{13}$  equivalent 1 Mev electrons/cm<sup>2</sup>. Array power output at the end of 5 years is 82.8 w/m<sup>2</sup>. Total array power is 6372 watts and is allocated as shown in Table 24. The total array area is 82.4 m<sup>2</sup>. Its weight breakdown is estimated in Table 25.

### Power Distribution Assemblies

Each power distribution assembly (PDA) contains 20 RPCs rated at 270 Vdc and 2 amperes. Command and telemetry circuits for the RPCs and buses are included. Ten separate 319-watt array sections are fed to the power processors through individual RPCs. Two sets of ten RPCs are provided to crosstie the array to the power processors as shown in Figure 19. Only one power processor is operating at a time from each PDA. The current through each RPC is 1.4 amperes at 240 Vdc and is kept below the 2 ampere rating by the inherent current limiting

Table 24. Power Allocation

Item	Power (Watts)	Bus (Volts)
Power processors	6000	240
Power processor control	140	28 ±7
RPC power distribution loss	100	240
RPC control	12	28 ±7
Telemetry and command	4	28 ±7
Battery charging	100	28 ±7
Miscellaneous losses	16	
Total	6372	

Table 25. Solar Array Weight Summary

Item	Weight	
	(kg)	(lb)
Mast	31.5	69.4
Guidewire	5.6	12.3
Mast tip	1.5	3.3
Cover	9.0	19.8
Container	10.1	22.2
Support struts	2.0	4.4
Array blankets	67.0	147.6
Harness	5.5	12.1
Miscellaneous hardware	2.0	4.4
Total	134.2	295.5

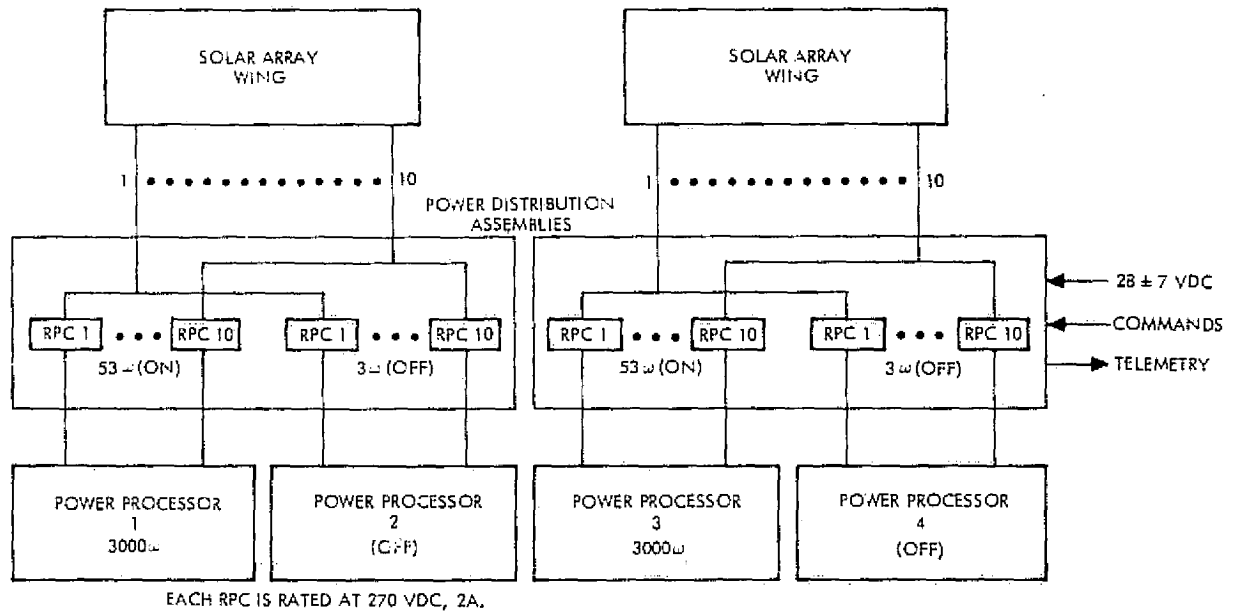


Figure 19. Electrical Power Interface

characteristic of each array section. RPC power dissipation is 5 watts (each) when conducting with 0.3 watt per RPC allocated to control circuits. Total heat dissipation per PDA is 58 watts, including command and telemetry circuit losses.

#### Battery Sizing

If the low voltage control circuits are kept on during eclipse, calculations show that the total energy supplied during eclipse is well within existing MMS battery capabilities at 6.6 Wh/kg energy density and 25% depth-of-discharge, which are consistent with a 2.5 year resupply interval for sun-synchronous satellite module servicing.

#### Power Subsystem Weight Summary

The weight attributable to the power subsystem for the propulsion module is presented in Table 26.

#### 3.2.7 Net Weight Impact

The net weight impact of the propulsion module for sun-synchronous satellite servicing is shown in Table 27. Propulsion subsystem dry weight data are presented in Section 3.2.4. Power subsystem weight impact is presented in Section 3.2.6. Thermal control and module structure weight estimates are 30.7 pounds (13.9 kg) and 96.6 pounds (43.9 kg), respectively.

Table 26. Power Subsystem Weight Attributable to the Propulsion Module

Item	Weight	
	(kg)	(lb)
Solar array wings	134.2	295.6
Power distribution assemblies	11.4	25.1
Added MMS harness	5.0	11.0
Array orientation mechanisms	13.6	30.0
Array harness	6.8	15.0
Total	171.0	376.7

Table 27. Net Weight Impact of Propulsion Module for Sun-Synchronous Satellite Servicing

Item	Weight	
	(kg)	(lb)
Ion propulsion subsystem	180.4	397.2
Propellant (includes 15% contingency reserve)	207.0	455.9
Additional power subsystem weight	171.0	376.7
Thermal control	13.9	30.7
Module structure	43.9	96.6
Total	616.2	1357.1

For comparison, a four-tank version of the hydrazine SPS-II propulsion module would be required for sun-synchronous satellite servicing. This module would weigh about 4500 pounds (2043 kg). Thus, an additional 3143 pounds (1427 kg) would be available for payload if the ion propulsion module were used instead.

### 3.3 COST ELEMENTS

Ion propulsion module costs for sun-synchronous satellite servicing are listed in Table 28. As before, start-up costs have been excluded from the estimates shown.

Nonrecurring costs assume a 2-1/2 year time span for development and qualification. Environmental and EMC tests are performed at the subsystem component level and the spacecraft system level. By virtue of module symmetry, only one propulsion half-system (using a full sized propellant tank) is required for development, and another propulsion half-system for qualification. Development testing at the subsystem level includes thermal-vacuum and thrusters/power processors integration tests. It is assumed that a Government facility will be used for the latter integration tests. Facility costs have been excluded from the estimates shown. Qualification testing at the subsystem level includes thermal-vacuum and mission duty cycle tests. The mission duty cycle is performed with a single thruster/power processor combination.

Table 28. Baseline Ion Propulsion Module Cost Breakdown

Item	Nonrecurring Costs (\$ millions)	Recurring		
		Unit Cost (\$ millions)	Quantity	Total (\$ millions)
Hardware				
Thruster and Gimbal Assembly	1.133	0.274	4 ea	1.096
Propellant Storage and Distribution	0.367	--	1 set	0.079
Power Processing Unit	4.826	0.308	4 ea	1.232
Thermal Control	0.480	--	1 set	0.255
Structure	0.280	--	As req'd	0.058
Integration and Assembly	0.338	--	As req'd	0.236
Solar Array	1.265	--	82.4 M <sup>2</sup>	1.725
Power Distribution Assembly	0.120	0.060	2 ea	0.120
Programmatic				
Aerospace Ground Equipment	1.969			0.007
Launch Operations	0.025			-0-
Development Tests	0.060			-0-
Qualification Tests	0.092			-0-
Subsystem Engineering	0.266			0.017
Reliability and Quality Assurance	0.128			0.336
Project Management	0.987			0.449
Total	12.336			5.610

Cost estimates for the 30-cm thruster and gimbal assembly are based on a recent Hughes study (Reference 25). Propellant storage and distribution costs are based on TRW experience with fluid components for similar spacecraft applications. Power processing unit costs are based on detailed costing data generated for Reference 10, and on parts comparisons. Power distribution assembly costs are based on TRW experience with electronics equipment. Thermal control cost estimates are based on similarity to previously built heat pipes for the TRW Independent Research and Development (IR&D) program, and on similarity to the radiator and insulation blanket for the CTS spacecraft. The estimates for structure, integration and assembly costs are based on Rockwell International analysis of hydrazine propulsion modules for MMS (Reference 11), adjusted to 1978 dollars, with provision for added electronics integration complexity. Solar array costs are based on Lockheed data from Reference 12.

AGE for the ion propulsion module primarily consists of power processor module test equipment, input controllers for the power processor, and ion engine load simulators. Subsystem engineering, reliability, and quality assurance costs listed under programmatic costs comprise those costs not included previously under component engineering and product assurance. Again, subsystem quality assurance and project management costs were derived parametrically.

### 3.3.1 Hardware Cost Factors

Examination of Table 28 shows that the largest hardware cost elements are in the solar array, power processor, and thruster. The cost of power in space is the subject of intensive development work at present, as is discussed further in Section 4.2. Power processing and thruster hardware costs have been discussed previously in Section 2.4.1.

Additional data on 30-cm ion thruster and power processor hardware may be found in References 17 through 20.

### 3.3.2 Sensitivity Analysis

The results from the sensitivity analysis conducted for the ion propulsion module are shown in Table 29. The MMS mission model in Reference 1 indicates 11 sun-synchronous missions. Accordingly, the sensitivity

Table 29. Sensitivity of Total Cost to Ion Propulsion Module Cost Elements

Item	n = 1		n = 5		n = 10	
	NR	R	NR	R	NR	R
Hardware						
Thruster and Gimbal Assembly	0.68	0.71	0.30	<u>1.57</u>	0.18	<u>1.85</u>
Propellant Storage and Distribution	0.22	0.05	0.10	0.11	0.06	0.13
Power Processing Unit	<u>2.90</u>	0.79	<u>1.29</u>	<u>1.76</u>	0.76	<u>2.08</u>
Thermal Control	0.29	0.16	0.13	0.36	0.08	0.43
Structure	0.17	0.04	0.07	0.08	0.04	0.10
Integration and Assembly	0.20	0.15	0.09	0.34	0.05	0.40
Solar Array	0.76	<u>1.11</u>	0.34	<u>2.47</u>	0.20	<u>2.91</u>
Power Distribution Assembly	0.07	0.08	0.03	0.17	0.02	0.20
Programmatic						
Aerospace Ground Equipment	<u>1.18</u>	<0.01	0.53	<0.01	0.31	0.01
Launch Operations	0.02	<0.01	<0.01	<0.01	<0.01	<0.01
Development Tests	0.04	<0.01	0.02	<0.01	<0.01	<0.01
Qualification Tests	0.06	<0.01	0.02	<0.01	0.01	<0.01
Subsystem Engineering	0.16	0.01	0.07	0.02	0.04	0.03
Reliability and Quality Assurance	0.08	0.20	0.03	0.45	0.02	0.53
Project Management	0.55	0.25	0.24	0.56	0.14	0.66

Sensitivity (%) of total cost to a 10% change in each cost element is listed for

n = number of modules required

NR = nonrecurring element

R = recurring element

analysis was performed for 1, 5, and 10 modules. In Table 29, the sensitivity to total cost for a 10% change in each cost element is shown. Wherever sensitivity exceeds 1%, it is underlined on the table.

### 3.4 BASELINE COMPARISON WITH SPS

Table 30 compares the baseline ion module for sun-synchronous satellite servicing with a four-tank version of SPS-II that would be required to do the same job. The recurring cost estimate for the SPS module was taken from Reference 1 (and adjusted to 1978 dollars). Shuttle charges for the ion module were determined from load factor by length. Shuttle charges for SPS were determined from load factor by weight, because its weight factor was greater than its load factor. The baseline comparison shows that ion module recurring costs are \$2.377 million more than a four-tank version of SPS-II.

Table 30. Baseline Ion Propulsion Module Comparison with SPS-II

	ION MODULE	SPS-II (4 TANK VERSION)
WEIGHT, KG (LB)	616 (1357)	2043 (4500)
Δ WEIGHT, KG (LB)	1427	(3143)
LENGTH, INCHES	27	60
Δ LENGTH, INCHES (FT)	33	(2.75)
RECURRING COST, \$M	5.610	1.387
PROPELLANT COST, \$M	0.002	0.019
SUB-TOTAL	5.612	1.406
SHUTTLE CHARGES FOR 160 N. M1. (a), \$M	6.088	7.917 (b)
TOTAL	11.700	9.323
Δ COST, \$M	(2.377)	

(a) ASSUMES 6 FT. LONG PAYLOAD

(b) LOAD FACTOR BY WEIGHT IS GREATER THAN LOAD FACTOR BY LENGTH



### 3.5 COST REDUCTION STUDIES

From the discussion in the proceeding sections, it is clear that the cost drivers for the ion propulsion module are:

- Shuttle charges
- Solar array
- Power processing
- Thruster and gimbal assembly

In order to investigate means for reducing the impact of these costs drivers, a series of cost reduction tradeoffs was conducted. Table 31 lists the studies performed. Each one is discussed separately below.

#### 3.5.1 Array Power Sharing

Most of the ion propulsion load power is taken from a 200 Vdc (minimum) solar array bus. The MMS bus furnishes 28 Vdc power. In order to share propulsion power with the payload (note: propulsion power is required primarily for orbit transfer maneuvers and only briefly on-orbit), either the solar array has to be reconfigured or additional power processing has to be provided to convert from 200 to 28 Vdc. A simple reconfiguration system was devised for power sharing, and was found preferable to additional power conversion equipment.

Table 31. Ion Propulsion Module Cost Reduction Studies

<u>Designation</u>	<u>Description</u>
30-1	Array Power Sharing
30-2	Thrust Throttling
30-3	Direct Drive (3-grid thrusters)
30-4	PPU Output Switching
30-5	Combination of 30-2 and 30-4
30-6	Extended Sun-Synchronous Mission: Change of Local Crossing Time

The solar array reconfiguration system between 200 and 28 Vdc is illustrated in Figure 20. It uses existing 28 Vdc, 20 ampere power relays. In Figure 20, all relay contacts are shown for 200 Vdc solar array output. The relays are transferred one at a time, starting at S1 and finishing at S12, to put all solar array sections in parallel for 28 Vdc output. To reconfigure for 200 Vdc output, the relays are transferred in reverse order starting at S12 and finishing at S1. The relays are switched sequentially in order not to exceed their voltage rating.

Figure 21 shows the block diagram for the power relay control electronics. It shows the relay drive, control logic, and optical coupler which transfer command signals and other solar array section relay electronic status signals to assure that the relays are transferred in the correct sequence. The control logic does not permit any relay contact to break more than a single solar array section voltage (nominally 28 Vdc). Each relay is isolated from ground to eliminate possible internal voltage stress. The relay drive electronics and drive power are also floating at solar array section potential ( - ). The command signals are optically coupled in order to latch each relay in either of two different states.

The power relay control unit will weigh an estimated 7.0 kg (15.4 lb). It has a standby power loss of 1.5 watts. During relay sequencing, its input power requirement increases to 6.9 watts.

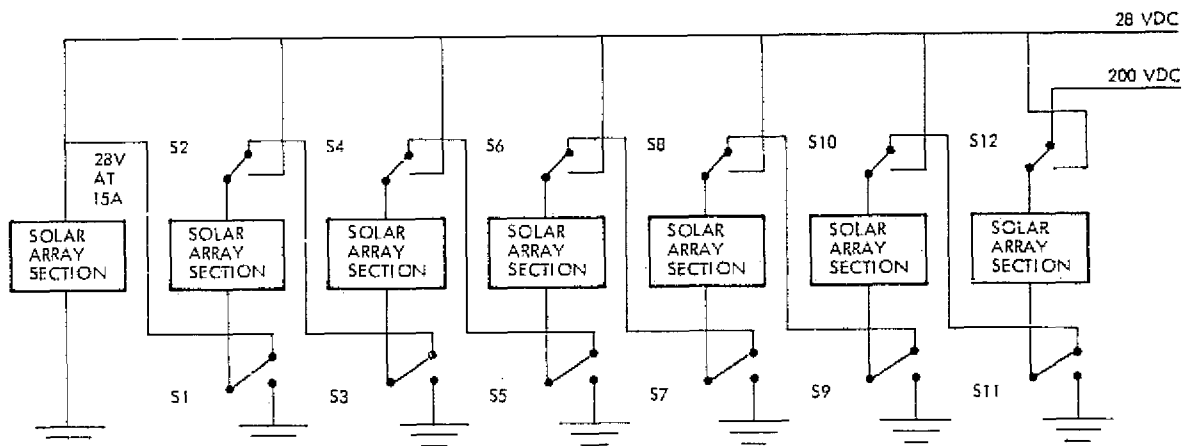


Figure 20. Solar Array Reconfiguration

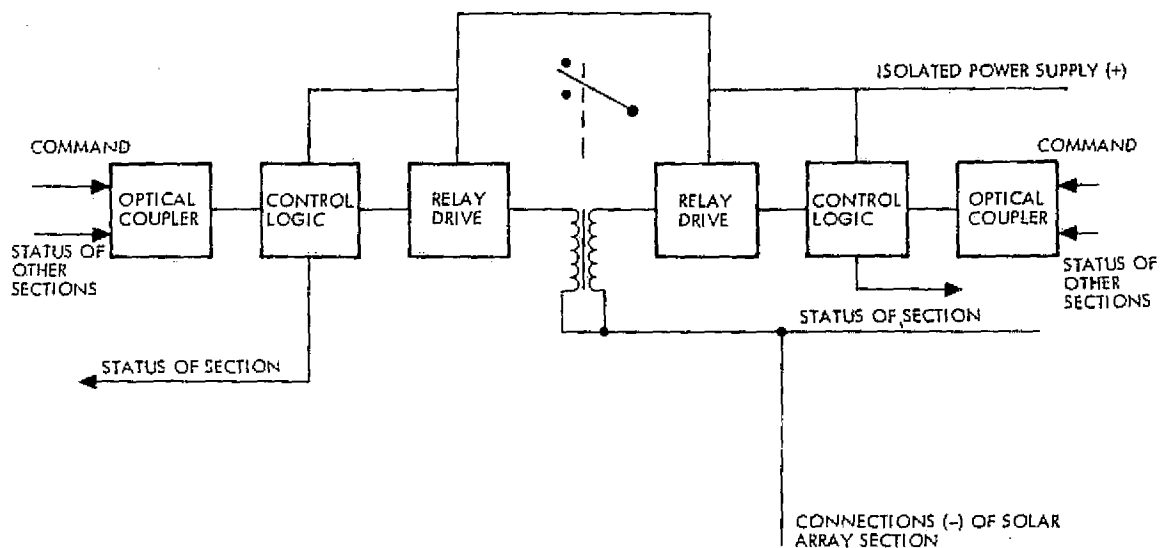


Figure 21. Block Diagram of Power Relay Control Electronics

The nonrecurring cost for reconfiguring the solar array is \$464 thousand. The recurring unit cost is \$102 thousand. In this manner, up to 3.6 kW can be shared with the standard MMS power module (described in Reference 26). For power sharing above 3.6 kW, another power module must be added to the spacecraft.

### 3.5.2 Thrust Throttling

The 30-cm thruster may be throttled to operate at reduced input power requirement. Performance in the throttled mode is documented in Reference 27. For example, by reducing the thruster beam current from 2 to 1 ampere, the engine produces 65.5 mN (14.7 mlb) thrust, about half of its full thrust capability. Thus, the powered portions of the orbit transfer maneuvers (the baseline trajectories include both powered and coast phases) will probably take twice as long as before, even though the total maneuver remains the same. The additional thrusting time is well within thruster design life capability. The trajectory analysis to precisely define the orbital maneuvers were beyond the scope of this present study effort.

The input power to the power processing unit (PPU) for operating the thruster at 1 ampere beam current is reduced to 1595 watts (from a baseline 3014 watts). The PPU weight decreases 8.0 kg (17.6 lb) from before, and its heat loss is reduced from 354 to 242 watts. The nonrecurring cost

reduction in the PPU, its related ground equipment, and the PDA (in the power subsystem) is \$262 thousand.

The recurring ion module cost reduction from the baseline is \$981 thousand. Most of the reduction is in solar array recurring cost.

### 3.5.3 Direct Drive (3 - Grid Thrusters)

Another way to reduce the thruster input power requirement is to add a third grid electrode (Reference 28), which permits the thruster to be operated at 400 volts screen potential and a 3 ampere beam current. The thruster then operates at 116 mN (26.1 mlb) thrust, about 10% less than baseline, and 1820 seconds specific impulse, versus 2900 seconds baseline. If it is assumed that a 400 Vdc solar array will have only minor interactive effects with the spacecraft and its surrounding plasma, then the array may be coupled directly to screen potential, eliminating the high power screen supply in the power processing unit. The concept of operating the screen grid directly from the solar array output is termed direct drive.

Since the screen supply is eliminated in direct drive, ion engine fault clearing must be accomplished differently than before. During fault clearing, the power subsystem RPC must be commanded open, and then the accelerator must be turned on followed by the reclosure of the main line RPC in order to reform the ion beam.

For the thruster operating conditions described above, the PPU input power is reduced to 2120 watts (from 3014 watts baseline). Its part count is reduced from 2312 to 1959 parts, and its weight decreases 8.6 kg (18.9 lb). The PPU heat loss is reduced from 354 to 205 watts.

Nonrecurring costs for direct drive were not estimated at the present time because of the early state of development. The thruster is presently being characterized under these operating conditions at the NASA-Lewis Research Center.

The recurring ion module cost reduction is estimated at \$963 thousand.

#### 3.5.4 PPU Output Switching

In a manner similar to that discussed for the HPPM, a high voltage relay network as shown in Figure 11 (Section 2.6.3) enables three power processors to operate four thrusters. The net effect eliminates one PPU from the ion module, and adds an output switch box containing 44 relays. The switch box weighs 3.7 kg (8.1 lb), and requires 27.5 watts to hold each set of relays (there are 11 relays in one set) closed. Thus, to operate both redundant thrusters and the redundant PPU simultaneously requires an additional 82.5 watts. The nonrecurring cost for the switch box is \$108 thousand. The unit recurring switch box cost is \$27 thousand.

The resulting recurring ion module cost reduction for incorporating an output switch box is \$340 thousand.

#### 3.5.5 Thrust Throttling and PPU Output Switching

The recurring cost breakdown in Table 32 is presented for incorporating thrust throttling and PPU output switching in the ion module. The combination of these cost reductions amounts to an ion module recurring cost of \$4.134 million for a \$1.296 million total reduction.

Referring to Table 30, it is seen that baseline ion module costs are \$2.377 million more than a four-tank version of SPS-II. By incorporating the cost reductions identified above, ion module recurring costs are \$1.081 million more, including propellant and Shuttle charges.

The ion module in this configuration (designation 30-5) makes 3.2 kW available for power sharing with the payload. The recurring cost increase for array reconfiguration per Section 3.5.1 is \$0.102 million. Cost elements in Table 31 directly associated with the power subsystem (solar array and power distribution assembly) total \$1.106 million. Thus, the recurring costs associated with power sharing almost balance the recurring cost difference between the ion module and SPS.

Table 32. Ion Module (Designation 30-5) Recurring Cost Breakdown

- Thrust throttling
- PPU output switching

Item	Unit Cost (\$ millions)	Quantity	Total (\$ millions)
Hardware			
Thruster and Gimbal Assembly	0.274	4 ea	1.096
Propellant Storage and Distribution	---	1 set	0.079
Power Processing Unit	0.297	3 ea	0.891
Thermal Control	---	1 set	0.194
Structure	---	As req'd	0.058
Integration and Assembly	---	As req'd	0.236
Solar Array	---	47 m <sup>2</sup>	1.026
Power Distribution Assembly	0.040	2 ea	0.080
Output Switch Box	0.027	1 ea	0.027
Programmatic			
Aerospace Ground Equipment			0.007
Subsystem Engineering			0.017
Reliability and Quality Assurance			0.258
Project Management			0.345
Total			4.314

### 3.5.6 Extended Sun-Synchronous Mission: Change of Local Crossing Time

An extended sun-synchronous mission is suggested in Reference 1 to take advantage of ion propulsion capability. The mission is based on the following assumptions:

- 1) A need exists for a satellite to alternate between different sun viewing conditions.
- 2) The satellite has the capability of returning to the Shuttle for servicing.
- 3) A transfer time of 3 months between viewing conditions is acceptable.
- 4) A single propulsion system is used for all main propulsion requirements.
- 5) Three transfers between the different viewing conditions are required.
- 6) Total mission life is at least 4 years.
- 7) The spacecraft and orbit are based upon the Landsat D/E mission.

An ion module containing six thrusters would be required to perform this mission. Chemically, an eight-tank version of SPS-II would be needed. Table 33 compares these two choices. From the comparison, it may be seen that the ion module recurring costs are \$0.990 million less than SPS, including propellant and Shuttle charges. Shuttle charges for the ion module were dominated by length, while the Shuttle charges for SPS were dominated by weight.

In order to perform this extended mission, each 30-cm ion thruster will have to cycle on and off from 3960 to 7085 times versus the present 3000 cycle design life. A shared cycling scenario may be devised to restrict thruster cycling to 4760 cycles each, which is still 1760 cycles above present design life. In order to qualify for this mission, the 30-cm thruster design life will have to be increased. For comparison, the 8-cm thruster design life is 10,000 cycles (Reference 16).

Table 33. Extended Sun-Synchronous Mission Comparison

	Ion Module, 6-Thruster Version	SPS, 8-Tank Version
Recurring Cost (\$M)	8.068	2.622
Propellant Cost (\$M)	0.006	0.042
Shuttle Charges (\$M)	6.088	12.488 (A)
Total	<u>14.162</u>	<u>15.152</u>
$\Delta$ Cost (\$M)	<div style="display: flex; align-items: center; justify-content: center;"> <div style="border-left: 1px solid black; width: 100px; height: 10px; margin-right: 5px;"></div> <div style="flex-grow: 1; border-bottom: 1px solid black; position: relative;"> <div style="position: absolute; left: 0; top: -5px; right: 0; border-top: 1px solid black;"></div> <div style="position: absolute; left: 0; top: -5px; right: 50px; border-top: 1px solid black;"></div> <div style="position: absolute; right: 0; top: -5px; left: 50px; border-top: 1px solid black;"></div> </div> <div style="margin: 0 10px;">→ 0.990 ←</div> </div>	

(A) Load factor by weight is greater than load factor by length.



#### 4. COST PROJECTION

Ion propulsion recurring costs, including the cost reductions studied, may be summarized as follows:

Synchronous HPPM	\$1.673 million
Low Earth Orbit HPPM	\$2.103 million
Ion Propulsion Module for Sun-Synchronous Satellite Servicing	\$4.314 million

Using the MMS mission model from Reference 1, however, it is apparent that nonrecurring ion propulsion costs cannot be paid back only via recurring cost savings when compared with hydrazine propulsion as provided by SPS-I and SPS-II. (Note: the mission model includes neither the extended HPPM nor the extended sun-synchronous missions.) In order to effectively absorb nonrecurring costs, the MMS mission model has to be expanded to take advantage of ion propulsion capability, or cost sharing with other ion propulsion programs must be implemented. The following discussion first identifies other programs that use ion propulsion. It then addresses recurring cost projections for the Shuttle era, which tend to increase the cost savings when compared with monopropellant hydrazine technology, because the latter technology is relatively mature, and will not benefit as much from advances in state of the art.

##### 4.1 ION ENGINE PROGRAMS

A number of programs using ion engines may, in the future, have sufficient commonality with MMS missions to permit nonrecurring cost sharing. The Air Force P80-1 satellite will have two 8-cm ion thruster subsystems on board as part of the SAMSO-601 flight test in 1981 (Reference 5). The SEPS (Solar Electric Propulsion Stage) program is entering Phase B in 1979 with a probable Phase C/D about a year later. It employs a 30 to 32 kW stage, utilizing approximately ten 30-cm ion engines. NASA-Lewis Research Center has an ongoing in-house technology development program, in both 8-cm and 30-cm thrusters. Commercial and military communications satellites are likely to take advantage of the payload benefits afforded by ion engine implementation (References 29 and 30).

Furthermore, advanced NASA planning activities for high power satellites and large space structures are engaged in studying ion engines for these applications.

#### 4.2 COST ELEMENT PROJECTIONS

In the Shuttle era, real cost reductions (neglecting inflation) for several ion propulsion cost elements are anticipated.

The cost of power in space is the subject of intensive development work. The SEPS array cost is estimated at \$240/watt (Reference 12). A reasonable projection for the megawatt array era is \$50/watt. Materials development work may reduce this even further to \$30/watt. NASA's goal is to reduce solar array cost to \$1/watt by the year 2000.

Batteries, on the other hand, are a mature technology, and cost reductions are not anticipated.

The thruster, propellant supply and distribution, and other mechanical hardware costs are primarily in assembly operations. An 80% learning curve is usually employed for such hardware (References 31 and 32). The thruster and gimbal assembly cost data presented in Reference 25 imply a 70% learning curve. Discussions with the thruster manufacturer indicate that gimbal mount simplification and tooling for larger quantity production will yield the largest cost reductions.

For power conditioning electronics, an 85% learning curve is typical. Also, other technology improvements will probably reduce actual costs an additional 25% by the year 2000. These improvements are expected in power component technology, automated testing, and standardization of component screening procedures. Widespread use of integrated circuits for control functions will also contribute. For example, a \$150 thousand nonrecurring investment to produce a regulator control LSI chip would reduce PPU recurring cost by \$10 thousand.

## 5. CONCLUSIONS

Ion propulsion recurring costs have been shown to compare favorably with the hydrazine propulsion modules on MMS for the following missions:

- Low earth orbit HPPM
- $\geq 4$  years geosynchronous HPPM
- Sun-synchronous mission requiring change in viewing conditions

For the low earth orbit mission, by incorporating cost reductions identified during the study, the HPPM recurring cost is \$0.600 million less than SPS-II, including propellant and Shuttle charges. Similarly, cost savings up to \$1.6 million have been identified for a 4-year geosynchronous HPPM mission. The ion propulsion module which was compared with SPS for the extended sun-synchronous mission indicates \$0.990 million lower recurring cost. Nonrecurring ion propulsion costs, however, must be shared with other programs unless the MMS mission model grows from that shown in Reference 1.

During the course of the study effort, ion propulsion cost drivers were identified as follows:

- Shuttle charges
- Solar array
- Power processor
- Thruster and gimbal assembly

Several design approaches to minimize the impact of these drivers on subsystem design were investigated. Cost effective design approaches included short length module configurations to minimize Shuttle charges. A simple solar array reconfiguration system was devised to permit power sharing with the payload. Operation at reduced thruster input power led to reduced solar array costs. This was achieved by thrust throttling or operation with three-grid thrusters. Simplified power processing units lowered hardware costs, while power processor output switching reduced the number of units required per subsystem.

The extended performance missions studied exhibited the greatest cost effectivity for ion propulsion when compared with monopropellant hydrazine subsystems.

## REFERENCES

1. N. H. Fischer and A. E. Tischer, "Study of Multimission Modular Spacecraft (MMS) Propulsion Requirements," NASA-GSFC Contract No. NAS7-786, August 8, 1977.
2. S. Zafran, ed., "Ion Engine Auxiliary Propulsion Applications and Integration Study," NASA CR-135312, NASA-Lewis Contract NAS3-20113, July 7, 1977.
3. "Low Cost Modular Spacecraft Description," (now called Multimission Modular Spacecraft) NASA Document X-700-75-140, Goddard Space Flight Center, May 1975.
4. "8-cm Mercury Ion Thruster Subsystem Users Manual," prepared by TRW for NASA-Lewis Research Center, July 1977.
5. J. L. Power, "Planned Flight Test of a Mercury Ion Auxiliary Propulsion System," AIAA Paper 78-647, April 1978.
6. B. G. Herron, et al, "Engineering Model 8-cm Thruster System," AIAA Paper 78-646, April 1978.
7. M. D. Thompson, "Failure Modes, Effects and Criticality Analysis," Summary Report for 8-cm Engineering Model Thruster System, NASA-Lewis Contract NAS 3-18917, July 1976.
8. J. M. Mansfield, F. G. Etheridge, J. Indrikis, "Landsat/MMS Propulsion Module Design," Final Report SD 76-SA-0095-2, NASA-Goddard Contract NAS 5-23524, September 24, 1976.
9. NASA-LeRC Data Package for MMS Study, Appendix B, Auxiliary Propulsion, March 1977.
10. J. J. Biess, L. Y. Inouye, and A. D. Schoenfeld, "Extended Performance Electric Propulsion Power Processor Design Study," NASA CR-135358, NASA-Lewis Contract NAS 3-20403.
11. F. Etheridge, W. Cooper, and J. Mansfield, "Landsat/MMS Propulsion Module Design," Rockwell International Space Division Report No. SD 76-SA-0095-3, September 24, 1976.
12. L. G. Chidester, "Advanced Lightweight Solar Array Technology," AIAA Paper 78-533, April 1978.
13. B. G. Herron, J. Hyman, Jr., and D. J. Hopper, "Development of an 8-cm Engineering Model Thruster System," AIAA Paper 76-1058, November 1976.
14. "STS Reimbursement Guide," JSC-11802, Final Review Copy, February 1978.

15. NASA Management Instruction 8610, "Subject: Reimbursement for Shuttle Services Provided to Non-U. S. Government Users," January 1977.
16. "Ion Propulsion for Spacecraft," NASA-Lewis Research Center, 1977.
17. T. D. Masek, R. L. Poeschel, C. R. Collett, and D. E. Snelker, "Evolution and Status of the 30-cm Engineering Model Ion Thruster," AIAA Paper 76-1006, November 1976.
18. J. E. Cake, G. R. Sharp, J. C. Oglebay, F. J. Shaker, and R. J. Zavesky, "Modular Thrust Subsystem Approaches to Solar Electric Propulsion Module Design," AIAA Paper 76-1062, November 1976.
19. J. J. Biess and R. J. Frye, "Electrical Prototype Power Processor for the 30 cm Mercury Electric Propulsion Engine," AIAA Paper 78-684, April 1978.
20. G. R. Sharp, L. Gedeon, J. C. Oglebay, F. J. Shaker, and C. E. Siegert, "A Prototype Power Management and Control System for the 30-cm Ion Thruster," AIAA Paper 78-685, April 1978.
21. J. J. Biess, L. Y. Inouye, and A. D. Schoenfeld, "Electric Prototype Power Processor for a 30-cm Ion Thruster," NASA CR-135287, NASA-Lewis Contract NAS 3-19730, March 1977.
22. G. R. Sundberg and W. W. Billings, "The Solid State Remote Power Controller: Its Status and Perspective," 1977 Power Conditioning Specialists Conference, IEEE, pp. 244-253.
23. R. V. Elms and L. W. Young, "SEP Full Scale Wing Development," 12th IECEC Proceedings, Vol. II, ANS, August 1977, pp. 1329-1334.
24. H. Y. Tada and J. R. Carter, "Solar Cell Radiation Handbook," NASA-JPL Publication 77-56, November 1, 1977.
25. R. L. Poeschel, E. I. Hawthorne, et al, "Extended Performance Solar Electric Propulsion Thrust System Study," NASA CR-135281, NASA-Lewis Contract NAS 3-20395, September 1977.
26. D. W. Harris, "The Modular Power Subsystem for the Multimission Modular Spacecraft," 13th IECEC Proceedings, Vol. I, SAE, August 1978, pp. 9-19.
27. R. T. Bechtel and V. K. Rawlin, "Performance Documentation of the Engineering Model 30-cm Diameter Thruster," AIAA Paper 76-1033, November 1976.
28. NASA-LeRC Data Package for Ion Propulsion Cost Effectivity Study, September 1978.

29. R. A. Meese, M. E. Ellion, and A. Burstein, "Application of Ion Engines to Synchronous Orbit Spacecraft," AIAA Paper 75-1229, September 1975.
30. D. H. Mitchell and S. Zafran, "Ion Propulsion for Spacecraft Reaction Control," AIAA Paper 78-651, April 1978.
31. H. Asher, "Cost-Quantity Relationships in the Airframe Industry," RAND R-291, July 1, 1956.
32. J. N. Lew, "Planning a General-Aviation Product," Aeronautics and Astronautics, Vol. 15, No. 1, January 1977, pp. 76-82.